Electronic Supplementary Material (ESI) for Analyst.

Supporting Information for

Electronically-tuned Triarylmethine Scaffold for Fast and Continuous Monitoring of H_2S Levels in Biological Samples

Ramshad Kalluruttimmal,[a] Divya Thekke Thattariyil,[b] Archana Panthalattu Parambil,[a] Ashis Kumar Sen, [c] Lakshmi Chakkumkumarath * [b] and Muraleedharan Kannoth Manheri * [a]

[a] Department of Chemistry, Indian Institute of Technology Madras

Chennai-600036, Tamil Nadu, India

e mail: mkm@iitm.ac.in

[b] Department of Chemistry, National Institute of Technology Calicut

Calicut-673601, Kerala, India

e mail: lakshmic@nitc.ac.in

[c] Mechanical Engineering, Indian Institute of Technology Madras,
Chennai-600036, Tamil Nadu, India.

Table of contents

1. Sensitivity of different triarylmethine dyes towards hydrogen sulfide

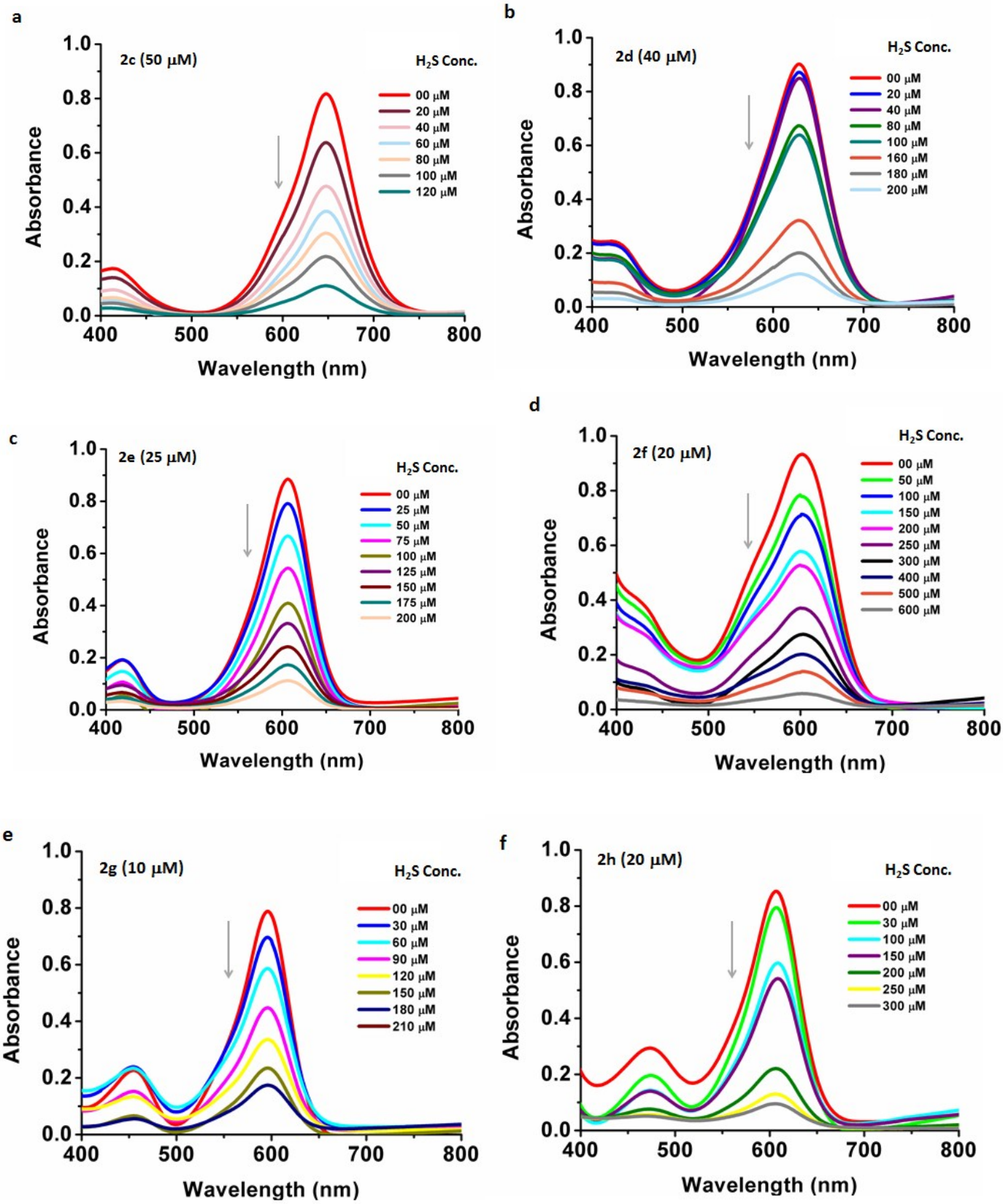

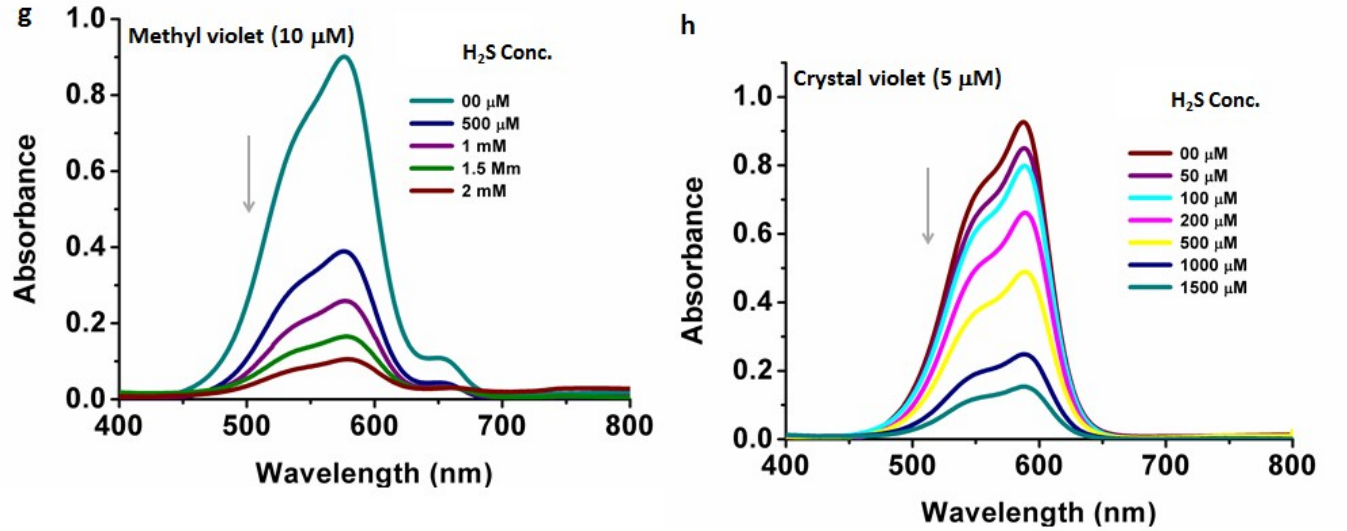

Figure S1. Change in absorbance of triarylmethine dyes on adding increasing amounts of H_2S.

Optimal probe concentrations for analysis and storage:

By studying different probe concentrations, we have found that if the water content is more than 98% there is a chance of small precipitation which leads to decrease in absorbance over a period of time. So, it is best to prepare the 1 mM stock solution in 1:1 ACN-Water mixture which gives same absorbance for extended period of time (monitored for a week). From this, aliquots can be withdrawn on requirement just before analysis as described in the manuscript)

2. Change in absorbance of triarylmethine dyes on reaction with two equivalents of H_2S

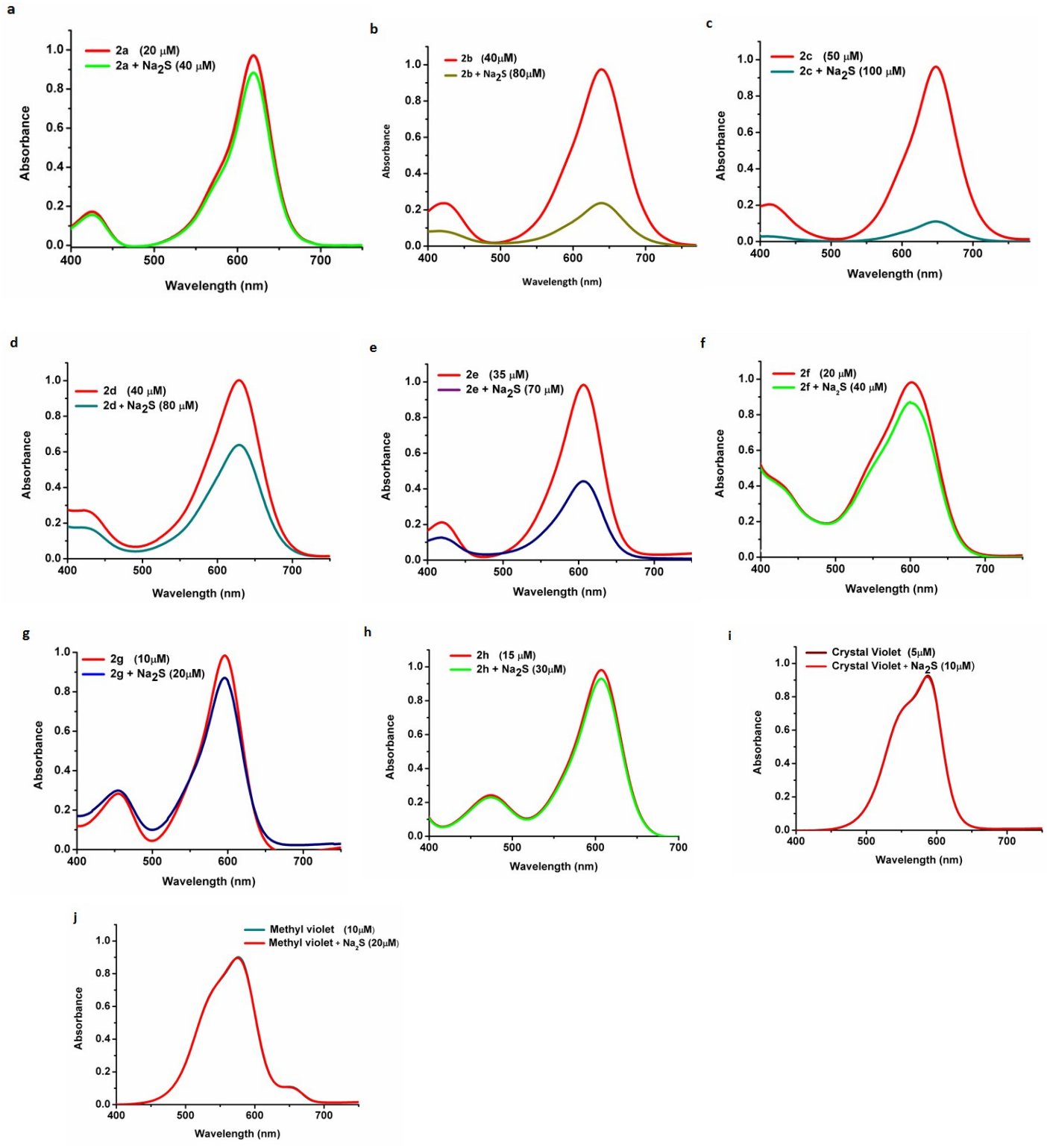

Figure S2. The decrease in absorbance of compounds **2a-h** on reaction with two equiv. of Na_2S

3. Response towards different anions

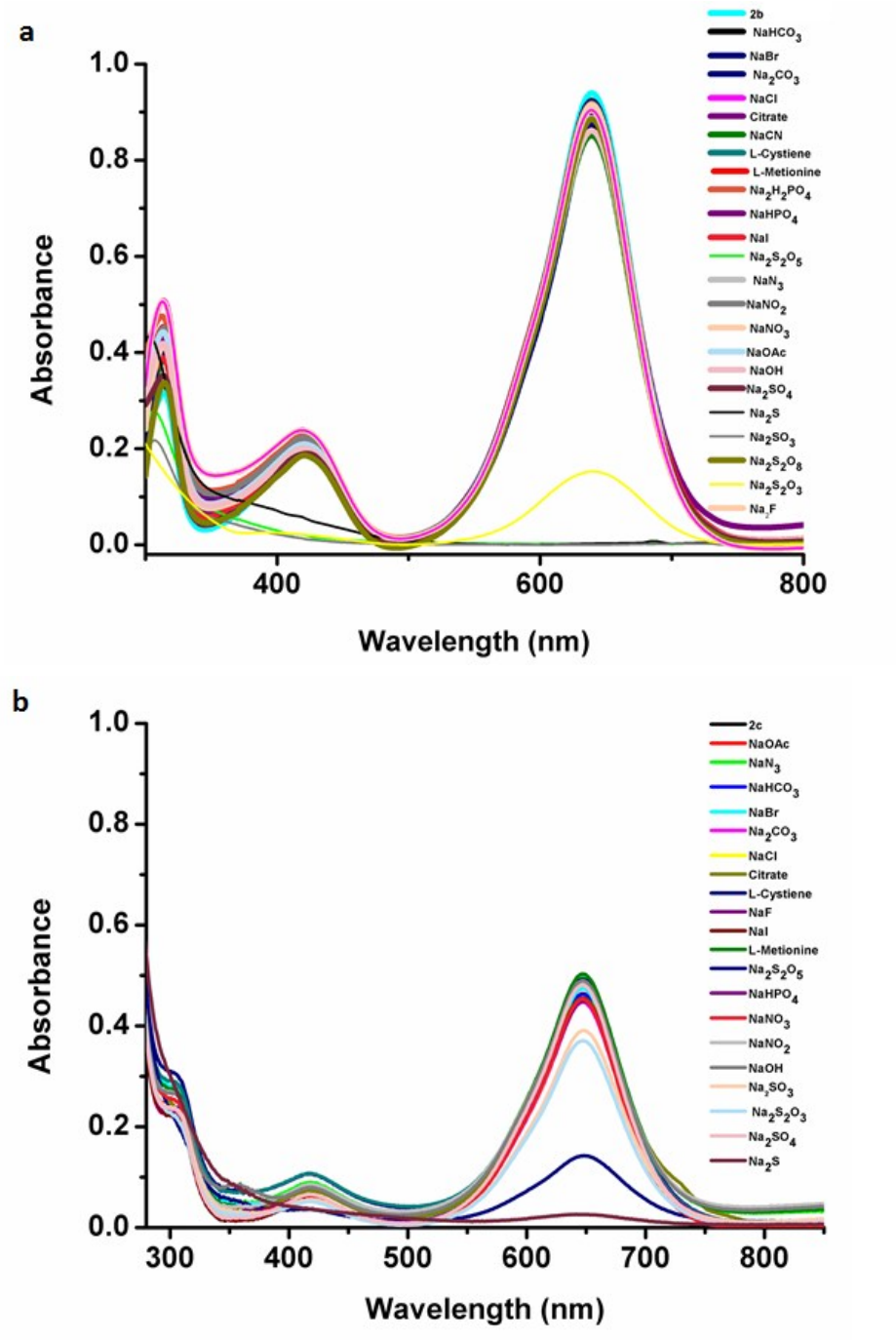

Figure S3. Change in the absorbance of a) compound **2b** (40 μM) and b) **2c** (30 μM) in presence of various analytes (10 mM)* in water-AcCN mixture (9:1 v/v, pH 7.4 at 25°C; *concentrations of N_3^-, CO_3^{2-} and OH^- taken were 1 mM each).

4. Effect of high bicarbonate and chloride concentrations on the absorption profile of **2b**.

a)

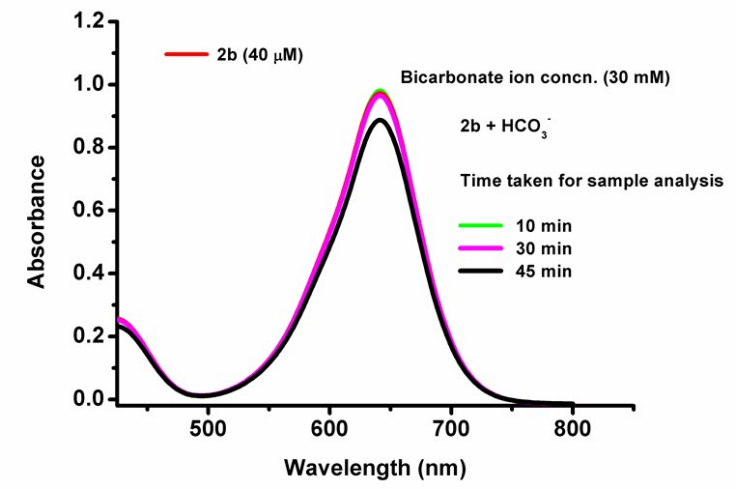

b)

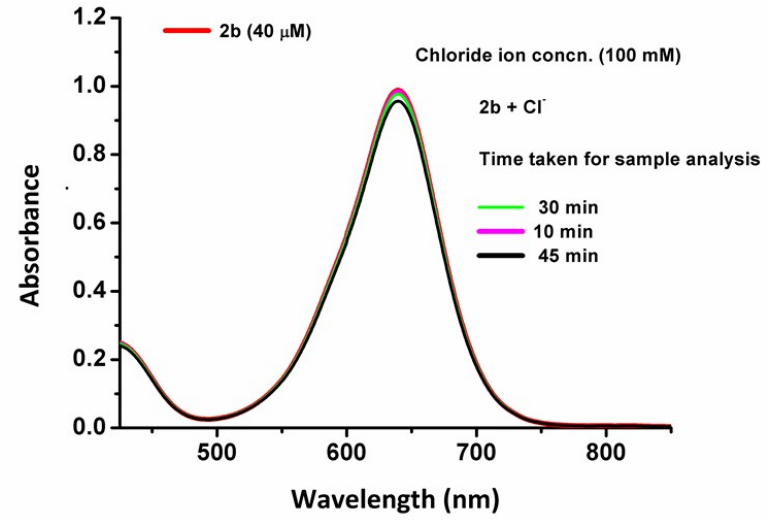

Figure S4. a) Absorbance of **2b** in presence of 30 mM concentration of bicarbonate at different time points. b) Corresponding spectra after treating with chloride ions at 100 mM concentration.

5. Reactivity of $Na_2S_2O_3$, $Na_2S_2O_5$, Na_2S and Na_2SO_3 with compounds **2b** and **2c**

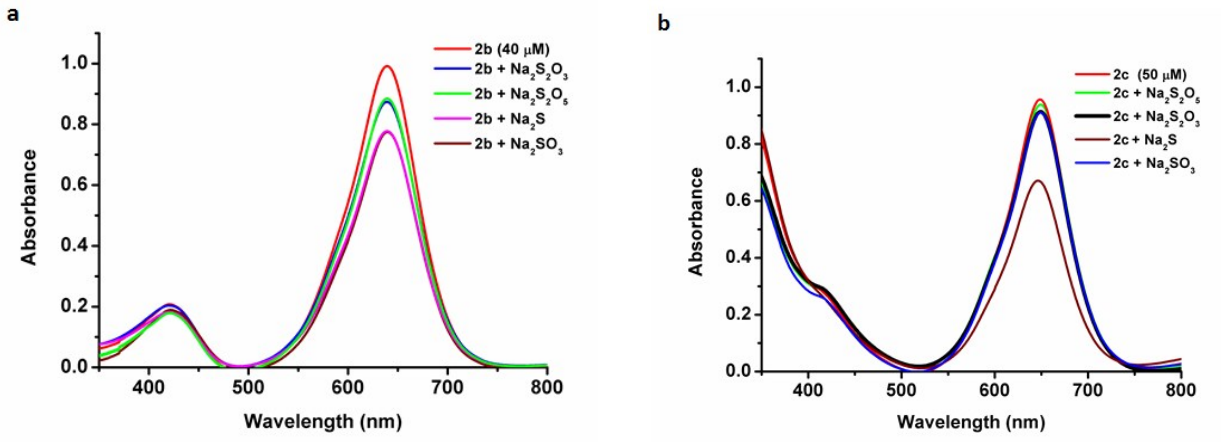

Figure S5. The absorption spectra of compounds a) **2b** (40 μM) and b) **2c** (50 μM) in presence of analytes such as $Na_2S_2O_3$, $Na_2S_2O_5$, Na_2S and Na_2SO_3 (20 μM).

6. Decolourisation and dye-regeneration steps involving **2c**

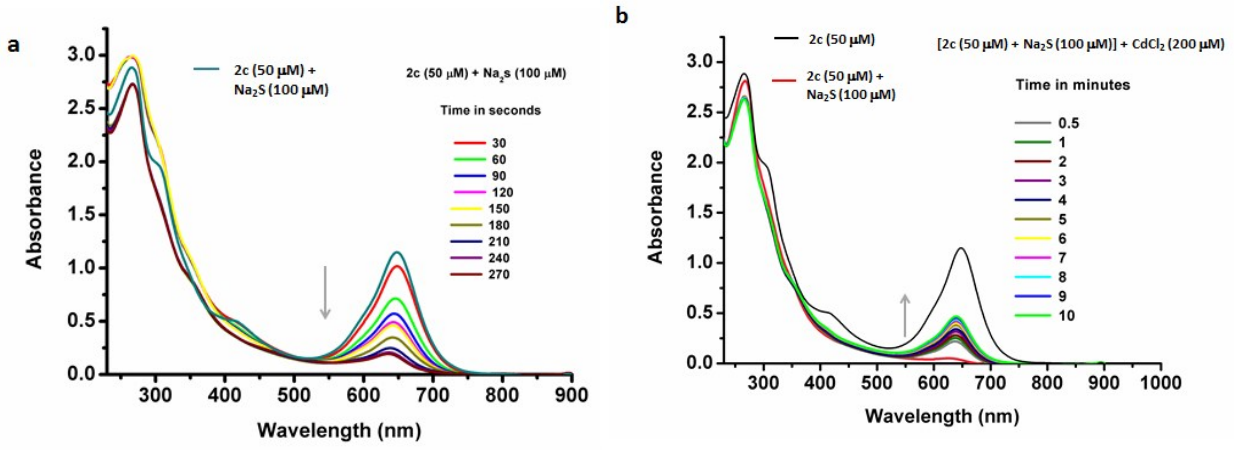

Figure S6. a) Time-dependent changes in the absorption spectra of compound **2c** in presence of H_2S and b) time-dependent changes in absorption spectra of **2c**-H_2S adduct on treatment with $CdCl_2$.

7. Time required for the regeneration of absorbance of **2b** in presence of $ZnCl_2$ and $CdCl_2$

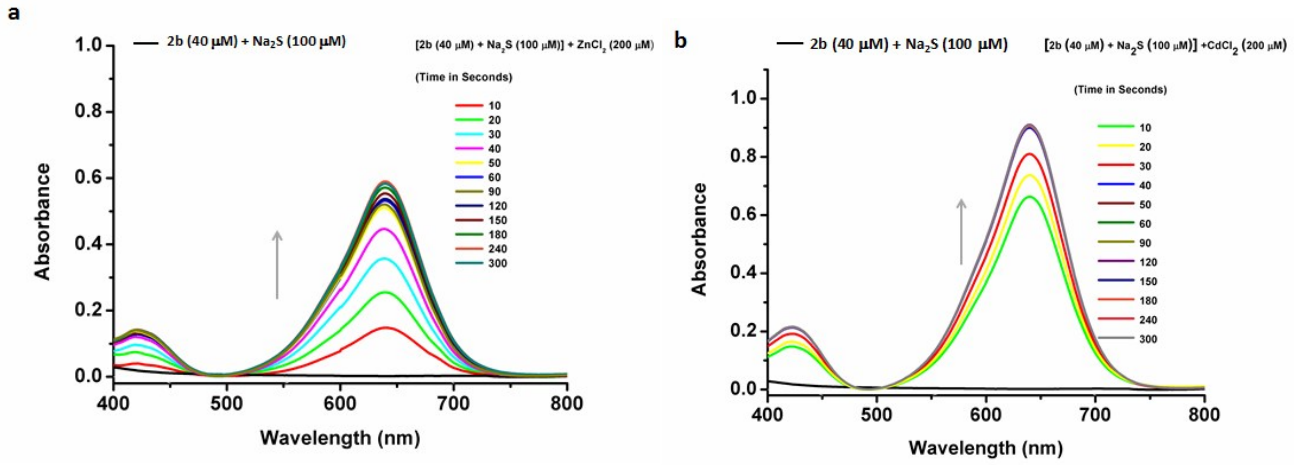

Figure S7. Time-dependent desulfuration of **2b-H_2S** adduct with a) $ZnCl_2$ and b) $CdCl_2$

8. Decolourisation and regeneration steps involving **2b** in saline condition (pH 6.8)

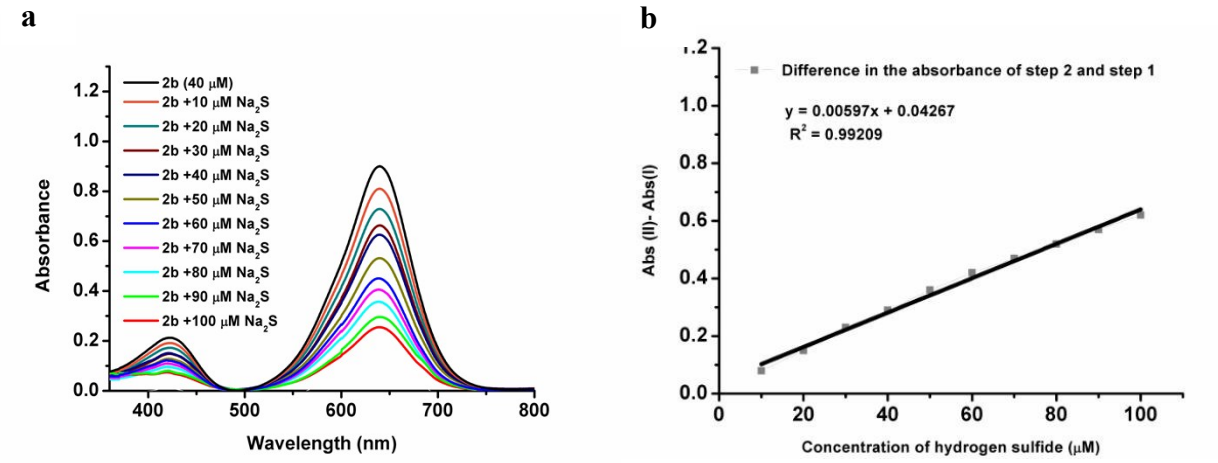

Figure S8. a) Change in the absorbance profile of **2b** (40 μM) in saline with increasing H_2S concentration. b) Linear change in absorbance due to dye regeneration on treatment with $CdCl_2$ (200 μM).

9. Effect of substitution on ring A on the absorption maxima of triarylmethine derivatives.

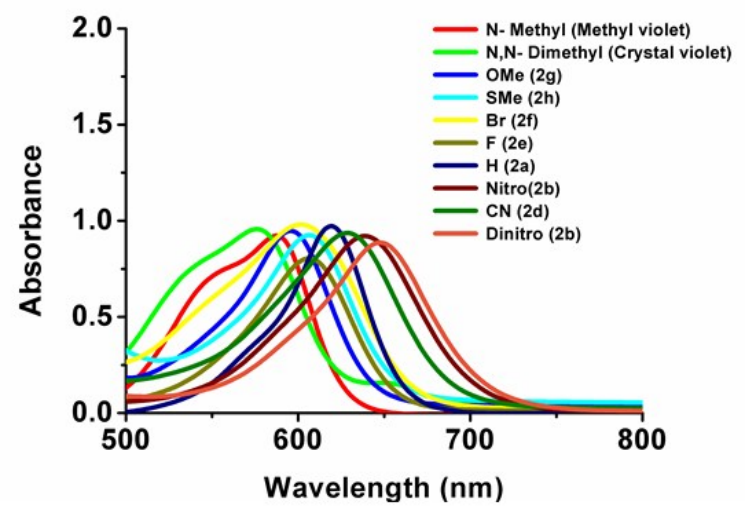

Figure S9. Shift in absorbance maximum of triarylmethine derivatives with change in substitution on ring A (concentrations of dyes as indicated in Figure S1)

10. Effect of increasing concentration of albumin on the absorption profile of **2b**

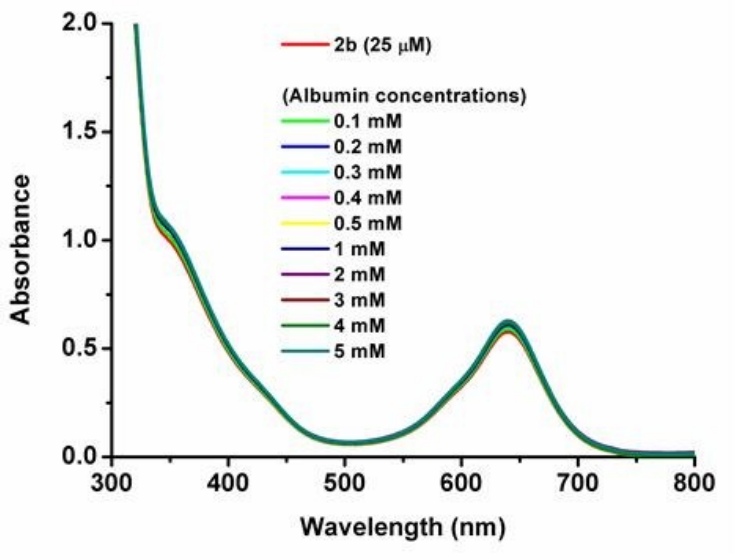

Figure S10. Absorbance of **2b** (25 μM) in presence of varying concentrations of albumin.

11. Change in absorbance of **2b** on treating Na_2S and $CdCl_2$ alternately

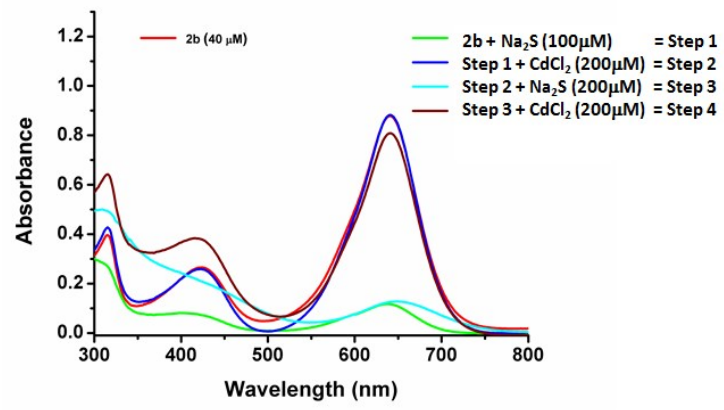

Figure S11. Absorbance spectra of **2b** (40 μM) on treatment with Na_2S and $CdCl_2$ solutions alternately at the concentrations indicated in the figure

12. Effect of polysulfide on the absorbance profile of **2b**

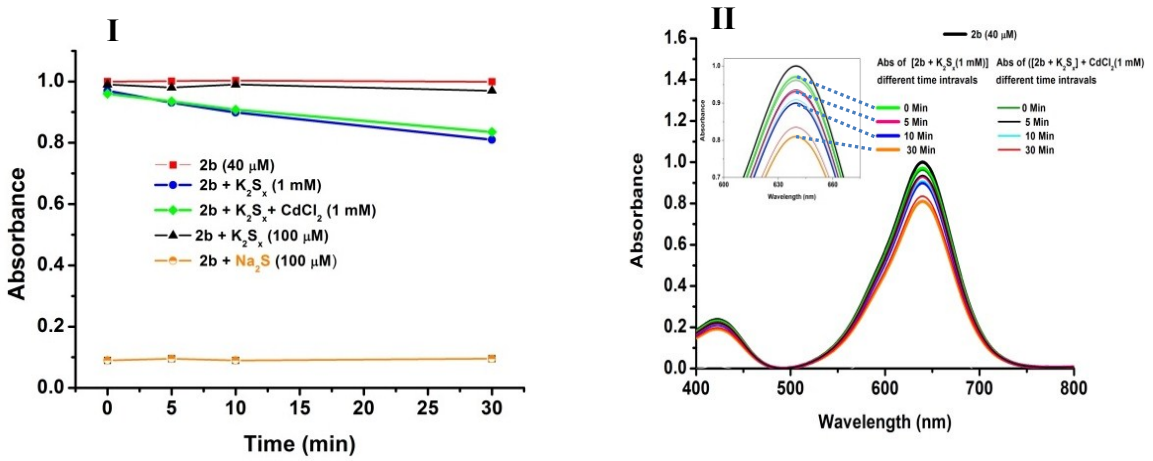

Figure S12. I. a) Time-dependant absorbance change of 2b (40 μM); b&c) Change in the absorbance profile of **2b** (40 μM) on addition of K_2S_x (1 mM) is shown in (b), whereas (c) shows that $CdCl_2$ treatment doesn't lead to dye-regeneration in this case; d) shows the response from 100 mM concentration of K_2S_x. e) the response from Na_2S (100 μM) is notably different and is included for comparison. The corresponding UV-Vis spectras are presented in **II.**

13. Reaction involved in the regeneration step

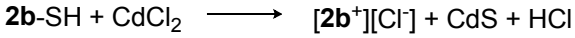

Figure S13. Scheme shows the reaction between sulfide adduct of **2b** with $CdCl_2$

14. Details of precision, accuracy, robustness etc.

Precision

The precision of a method is the closeness of independent test outcomes obtained under optimal conditions. Three different concentrations of Na_2S in the linear range (10, 20 and 30 μM) were analyzed in 3 independent runs in the same day (intra-day precision) and 3 successive days (inter-day precision) from three measurements of each sample. The precision of the analysis was determined by calculating the relative standard deviation (RSD %). The RSD values of intra-day and inter-day studies differ from 1.00 to 1.57 in buffer and 1.47 to 2.87 in plasma respectively. The intermediate precision of the method was satisfactory (ESI-Table 1).

ESI-Table 1. Intra-day and inter-day precision determined for different concentrations (10 μM, 20 μM and 30 μM) of analyte.

(Buffer)	**Intra-day precision**			**Inter-day precision**		
Concentration (μM)	Absorbance measured (Mean ± SD)	% RSD	± SE	Absorbance measured (Mean ± SD)	% RSD	± SE
10	0.0938 ± 0.00094	1.00	0.054	0.0887 ± 0.00111	1.24	0.06
20	0.1891 ± 0.00195	1.03	0.113	0.1816 ± 0.00188	1.04	0.11
30	0.2909 ± 0.00314	1.08	0.18	0.2756 ± 0.00433	1.57	0.25
(Plasma)	**Intra-day precision**			**Inter-day precision**		
Concentration (μM)	Absorbance measured (Mean ± SD)	% RSD	± SE	Absorbance measured (Mean ± SD)	% RSD	± SE
10	0.1851 ± 0.00404	2.18	0.23	0.1558 ± 0.00447	2.87	0.25
20	0.2535 ± 0.00625	2.46	0.36	0.2323 ± 0.00620	2.67	0.35
30	0.3328 ± 0.00558	1.68	0.32	0.2890 ± 0.00425	1.47	0.25

* Standard deviation (SD) = square root of $\sum (m-i)^2/n-1$ (m is the mean)

* Percentage relative standard deviation, $\%RSD = 100*(SD/m)$

* Standard error (SE) = Standard deviation/$\sqrt{n}$

Accuracy and recovery

Accuracy was determined based on data obtained for three different concentrations (n = 3) and the value is expressed as percentage of recovery between the mean concentrations of the analyte recovered and that of the original. The average recoveries were found to be as 100.6%, 99.2% and 100.7% in buffer and 101.4%, 101.7% and 98.6 in plasma for the concentration levels of 15, 20, 25 μM respectively (ESI-Table 2). Also the percentage relative error was less than 0.80 in buffer and 1.75 in plasma respectively.

ESI-Table 2. Determination of accuracy of data using 2b and the percentage recovery

(Buffer) **Concentration(μM)**		**% Average recovery (r)**	**% Relative error (δ)**
Amount added [C]	Amount Found ([C]$^{\#}$ ±SD)		
15	15.09 ± 0.1496	100.6	0.60
20	19.84 ± 0.1557	99.2	0.80
25	25.18 ± 0.1584	100.7	0.72
(Plasma)			
15	15.21± 0.5391	101.4	1.40
20	20.35 ± 0.8083	101.7	1.75
25	24.66 ± 0.8513	98.6	1.36

% Average recovery (r) = $100*[C]^{\#}/[C]$ % Relative error (δ) $=100*([C]^{\#}-[C])/[C]$

Robustness

Robustness of the method was assessed by taking measurements at slightly different wavelengths for detection and quantification (636 nm and 640 nm). All parameters except the wavelength were made constant during this study. Seven independent measurements using a 20 μM Na_2S solution was done at both these wave lengths. The statistical comparison was done with Friedman analysis and no significant difference was found between the results ($p = 0.087 > p = 0.05$ in buffer and $p= 0.7055 > p=0.05$ in plasma) (ESI-Table 3).

ESI-Table 3. The robustness data of current method (n=7).

(Buffer) Solution	**Found, (μM)**	**% RSD**
Standard, 20 (μM) at 638 nm	20.61±0.2223	1.07
Wavelength, 636 nm	20.63±0.2944	1.43
Wavelength, 640 nm	21.04±0.3123	1.48
Friedman analysis: p = 0.0878 > p = 0.05		
(Plasma) Solution	**Found, (μM)**	**% RSD**
Standard, 20 (μM)	20.81±0.3041	1.46
Wavelength, 636 nm	20.85±0.4131	1.98
Wavelength, 640 nm	21.27±0.3414	1.60
Friedman analysis: p = 0.7055 > p = 0.05		

(ref. G. L. Long and J. D. Winefordner, *Anal. chem*., 1983, **55**, 712)

Spectral data of 1 b- h and 2 b- h

1b: Yield, 92%; R_f (5% EtOAc-Hexane), 0.36; mp 144−146 °C; IR (KBr) ν_{max} 3000, 2793, 1884, 1607, 1516, 1443, 1336 cm^{-1}; ^1H NMR ($CDCl_3$, 400 MHz) δ 8.12-8.10 (2H, d, *J* = 8.48 Hz), 7.30-7.28 (2H, d, *J* = 8.45 Hz), 6.95-6.93 (4H, d, *J* = 8.15 Hz), 6.68-6.66 (4H, d, *J* = 8.15 Hz), 5.45 (1H, s), 2.93 (12H, s) ppm; ^{13}C NMR ($CDCl_3$, 100 MHz) δ 153.6, 149.4(2C), 146.3, 131.1(2C), 130.2(2C), 129.9(4C), 123.5(2C), 112.7(4C), 55.1, 40.7(4C) ppm; HRMS (ESI) exact mass calcd. for $C_{23}H_{26}N_3O_2$ $[M+H]^+$ 376.2042, found 376.2032.

1c: Yield, 93%; R_f (5% EtOAc-Hexane), 0.32; mp 160−162 °C; IR (KBr) ν_{max} 3000, 2796, 1880, 1607, 1516, 1445, 1344 cm^{-1}; ^1H NMR ($CDCl_3$, 400 MHz) δ 8.64 (1H, s), 8.27-8.25 (1H, d, *J* = 8.60 Hz), 7.40-7.37 (1H, d, *J* = 8.60 Hz), 6.90-6.88 (4H, d, *J* = 8.45 Hz), 6.66-6.63 (4H, d, *J* = 8.45 Hz), 6.11 (1H, s), 2.92 (12H, s) ppm; ^{13}C NMR ($CDCl_3$, 100 MHz) δ 149.6(2C), 147.3, 146.1, 133.4, 130.1(4C), 128.9(2C), 126.1, 120.1(2C), 112.7(4C), 50.0, 40.6(4C) ppm; HRMS (ESI) exact mass calcd. for $C_{23}H_{25}N_4O_4$ $[M+H]^+$ 421.1875, found 421.1843.

1d: Yield, 90%; R_f (5% EtOAc-Hexane), 0.36; mp 132−134 °C; IR (KBr) ν_{max} 3004, 2884, 2804, 2074, 1888, 1614, 1520, 1484, 1443 cm^{-1}; ^1H NMR ($CDCl_3$, 400 MHz) δ 7.55-7.53 (2H, d, *J* = 7.86 Hz), 7.25-7.23 (2H, d, *J* = 7.86 Hz), 6.94-6.92 (4H, d, *J* = 8.46 Hz), 6.68-6.65 (4H, d, *J* = 8.46 Hz), 5.40 (1H, s), 2.92 (12H, s) ppm; ^{13}C NMR ($CDCl_3$, 100 MHz) δ 151.4, 149.4(2C), 132.1(2C), 131.2(2C), 130.2(2C), 129.9(4C), 119.3, 112.7(4C), 109.7, 55.2, 40.7(4C) ppm; HRMS (ESI) exact mass calcd. for $C_{24}H_{26}N_3$ $[M+H]^+$ 356.2126, found 356.2134.

1e: Yield, 86%; R_f (5% EtOAc-Hexane), 0.34; mp 130−132 °C; IR (KBr) ν_{max} 3004, 2856, 2800, 1880, 1610, 1520, 1445 cm^{-1}; ^1H NMR ($CDCl_3$, 400 MHz) δ 7.09-7.07 (2H, dd, *J* = 8.07 Hz & 2.05 Hz), 6.98-6.92 (6H, m), 6.68-6.66 (4H, d, *J* = 8.63 Hz), 5.36 (1H, s), 2.92 (12H, s) ppm; ^{13}C NMR ($CDCl_3$, 100 MHz) δ 149.2(2C), 132.8, 130.9(2C), 130.8(4C), 129.9, 115.0(2C), 114.8(2C), 112.7(4C), 54.4, 40.8(4C) ppm; HRMS (ESI) exact mass calcd. for $C_{23}H_{26}FN_2$ $[M+H]^+$ 349.2080, found 349.2085.

1f: Yield, 83%; R_f (5% EtOAc-Hexane), 0.32; mp 136−138 °C; IR (KBr) ν_{max} 3004, 2800, 1884, 1610, 1516, 1347, 1221 cm^{-1}; ^1H NMR ($CDCl_3$, 400 MHz) δ 7.40-7.38 (2H, d, *J* = 8.13 Hz), 7.04-7.02 (2H, d, *J* = 8.13 Hz), 6.98-6.96 (4H, d, *J* = 8.33 Hz), 6.69-6.67 (4H, d, *J* = 8.33 Hz), 5.34 (1H, s), 2.93 (12H, s) ppm; ^{13}C NMR ($CDCl_3$, 100 MHz) δ 149.2(2C), 144.7, 132.2(2C), 131.2(4C), 129.9(2C), 129.5(2C), 119.8, 112.7(4C), 54.6, 40.8(4C) ppm; HRMS (ESI) exact mass calcd. for $C_{23}H_{26}BrN_2$ $[M+H]^+$ 409.1287, found 409.1276.

1g: Yield, 85%; R_f (5% EtOAc-Hexane), 0.39; mp 148−150 °C; IR (KBr) ν_{max} 3004, 2884, 2800, 1880, 1610, 1520, 1445, 1344 cm^{-1}; ^1H NMR ($CDCl_3$, 400 MHz) δ 7.05-7.03 (2H, d, *J* = 8.27 Hz), 6.99-6.96 (4H, d, *J* = 8.27 Hz), 6.81-6.79 (2H, d, *J* = 8.48 Hz), 6.68-6.65 (4H, d, *J* = 8.64 Hz), 5.33 (1H, s), 3.78 (3H, s), 2.91 (12H, s) ppm; ^{13}C NMR ($CDCl_3$, 100 MHz) δ 157.8, 149.1(2C), 137.8, 133.4(2C), 130.4(2C), 130.0(4C), 113.6(2C), 112.7(4C), 55.4, 54.3, 40.9(4C) ppm; HRMS (ESI) exact mass calcd. for $C_{24}H_{29}N_2O$ $[M+H]^+$ 361.2279, found 361.2261.

1h: Yield, 88%; R_f (5% EtOAc-Hexane), 0.38; mp 138−140 °C; IR (KBr) ν_{max} 3000, 2881, 2800, 1884, 1610, 1516, 1445, 1344 cm^{-1}; ^1H NMR ($CDCl_3$, 400 MHz) δ 7.19-7.17 (2H, d, *J* = 8.32 Hz), 7.08-7.06 (2H, d, *J* = 8.32 Hz), 7.00-6.98 (4H, d, *J* = 8.66 Hz), 6.69-6.67 (4H, d, *J* = 8.66 Hz), 5.35 (1H, s), 2.92 (12H, s), 2.46 (3H, s) ppm; ^{13}C NMR ($CDCl_3$, 100 MHz) δ 149.1(2C), 142.8, 135.4, 132.8(2C), 130.0(4C), 129.9(2C), 126.9(2C), 112.7(4C), 54.6, 40.8(4C), 16.3 ppm; HRMS (ESI) exact mass calcd. for $C_{24}H_{29}N_2S$ $[M+H]^+$ 377.2051, found 377.2060.

2d: Yield, 92%; R_f (5% MeOH-DCM), 0.56; mp 172−174 °C; IR (KBr) ν_{max} 3004, 2881, 2804, 1880, 1614, 1520, 1445, 1351 cm^{-1}; ^1H NMR (CD_3OD, 500 MHz) δ 7.94-7.92 (2H, d, *J* = 8.64 Hz), 7.53-7.51 (2H, d, *J*

= 8.64 Hz), 7.42-7.40 (4H, d, *J* = 8.46 Hz), 7.07-7.06 (4H, d, *J* = 8.46 Hz), 3.34 (12H, s) ppm; ^{13}C NMR (125 MHz, CD_3OD) δ 174.7(2C), 158.7, 141.6(4C), 135.7(2C), 133.3(2C), 131.3, 128.3(2C), 119.0, 115.3(4C), 113.4, 41.1(4C) ppm; HRMS (ESI) exact mass calcd. for $C_{24}H_{24}N_3$ $[M]^+$ 354.1970, found 354.1979.

2e: Yield, 86%; R_f (5% MeOH-DCM), 0.38; mp 152−154 °C; IR (KBr) ν_{max} 3007, 2891, 2804, 1884, 1610, 1526, 1347 cm^{-1}; ^{1}H NMR (400 MHz, D_2O) δ 7.28-7.22 (8H, m), 6.86-6.84 (4H, d, *J* = 8.66 Hz), 3.20 (12H, s) ppm; ^{13}C NMR (100 MHz, CD_3OD) δ 178.9(2C), 158.6, 141.9(4C), 141.1, 135.7(2C), 134.1, 129.7(2C), 128.5(2C), 114.8(4C), 40.9(4C) ppm; HRMS (ESI) exact mass calcd. for $C_{23}H_{24}FN_2$ $[M]^+$ 347.1923, found 347.1935.

2f: Yield, 89%; R_f (5% MeOH-DCM), 0.44; mp 146−148 °C; IR (KBr) ν_{max} 3007, 2796, 1884,1618, 1505, 1351 cm^{-1}; ^{1}H NMR (400 MHz, CD_3OD) δ 7.79-7.74 (2H, d, *J* = 8.13 Hz), 7.44-7.42 (4H, d, *J* = 8.13 Hz), 7.29- 7.27 (2H, d, *J* = 8.33 Hz), 7.08-7.06 (4H, d, *J* = 8.33 Hz), 3.34 (12H, s) ppm; ^{13}C NMR (100 MHz, CD_3OD) δ 176.1(2C), 158.6, 141.8(4C), 140.0, 137.1(2C), 133.1(2C), 129.0, 128.3(2C), 114.9(4C), 40.9(4C) ppm; HRMS (ESI) exact mass calcd. for $C_{23}H_{24}BrN_2$ $[M]^+$ 407.1122, found 407.1129.

2g: Yield, 91%; R_f (5% MeOH-DCM), 0.49; mp 188−190 °C; IR (KBr) ν_{max} 3014, 2811, 1891, 1607, 1512,1347 cm^{-1}; ^{1}H NMR (400 MHz, CD_3OD) δ 7.43-7.41 (4H, d, *J* = 8.48 Hz), 7.37-7.35 (2H, d, *J* = 8.27 Hz), 7.18-7.16 (2H, d, *J* = 8.27 Hz), 7.05-7.03 (4H, d, *J* = 8.48 Hz), 3.96 (3H, s), 3.31 (12H, s) ppm; ^{13}C NMR (100 MHz, CD_3OD) δ 179.7(2C), 166.4, 158.4, 141.9(4C), 138.9(2C),133.3, 128.3(2C), 115.6(2C), 114.4(4C), 56.5, 40.8(4C) ppm; HRMS (ESI) exact mass calcd. for $C_{24}H_{27}N_2O$ $[M]^+$ 359.2156, found 359.2146.

2h: Yield, 92%; R_f (5% MeOH-DCM), 0.38; mp 158−160 °C; IR (KBr) ν_{max} 2997, 2849, 2796, 1891, 1607, 1520, 1439, 1344 cm^{-1}; ^{1}H NMR (400 MHz, D_2O) δ 7.28-7.26 (2H, d, *J* = 8.27 Hz), 7.23-7.21 (4H, d, *J* = 8.27 Hz), 7.07-7.05 (2H, d, *J* = 8.48 Hz), 6.84-6.82 (4H, d, *J* = 8.48 Hz), 3.24 (12H, s), 2.55 (3H, s) ppm; ^{13}C NMR (100 MHz, DMSO-d_6) δ 156.4, 140.1(4C), 135.2, 129.5(2C), 129.4(2C), 126.3, 125.9(2C), 124.9(2C), 113.8(4C), 53.6, 40.5(4C) ppm; HRMS (ESI) exact mass calcd. for $C_{24}H_{27}N_2S$ $[M]^+$ 375.1894, found 375.1951.

^{1}H & ^{13}C NMR spectra of 1 b- h and 2 b- h

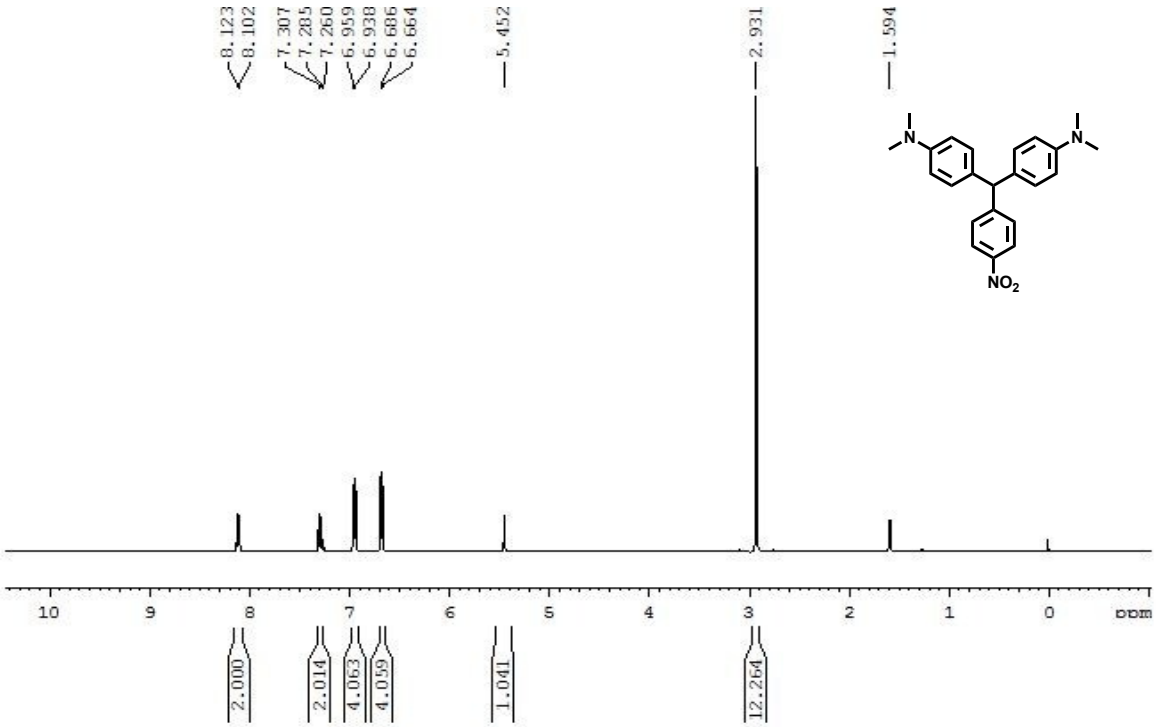

Figure S14. ^{1}H NMR spectrum (400 MHz, $CDCl_3$) of the compound **1b**

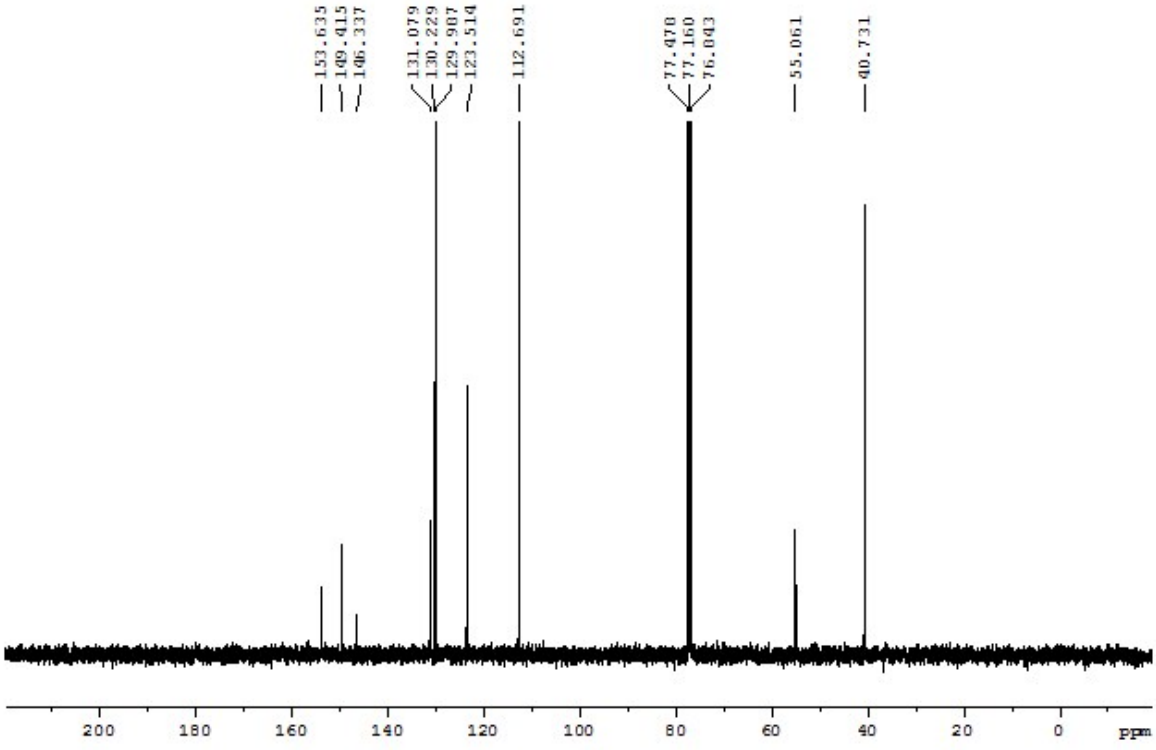

Figure S15. ^{13}C NMR spectrum (100 MHz, $CDCl_3$) of the compound **1b**

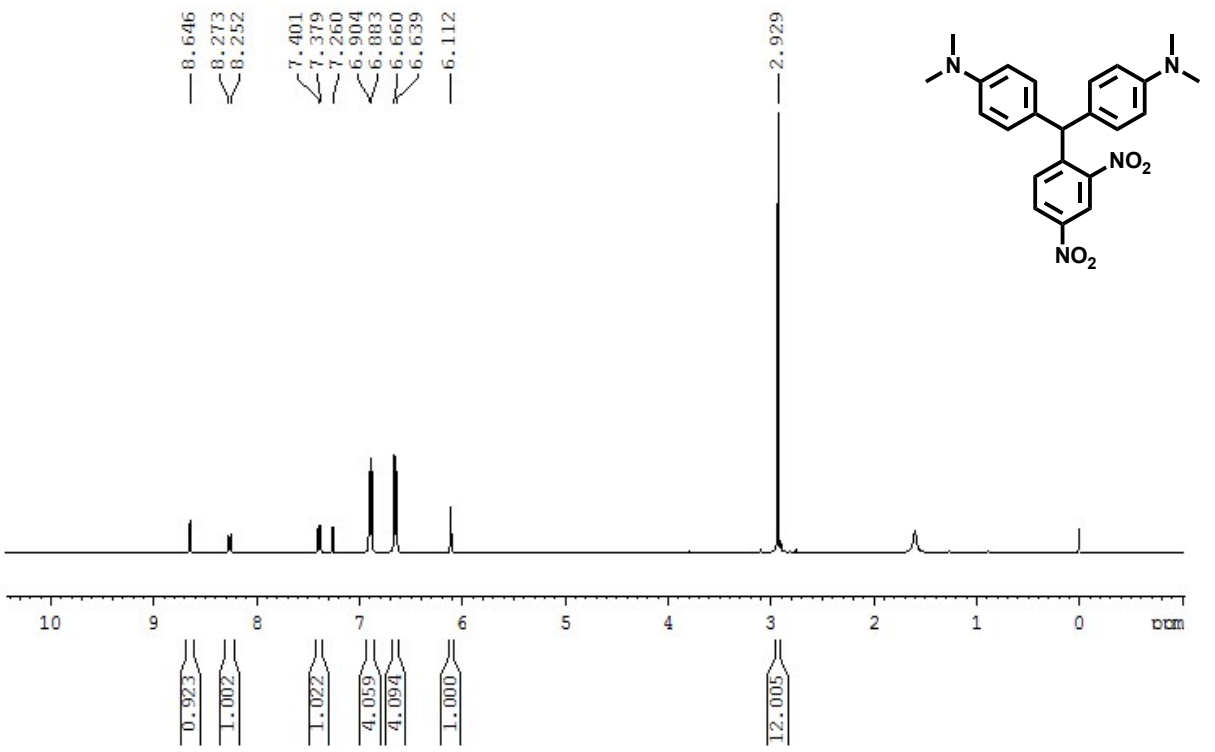

Figure S16. ^{1}H NMR spectrum (400 MHz, $CDCl_3$) of the compound **1c**.

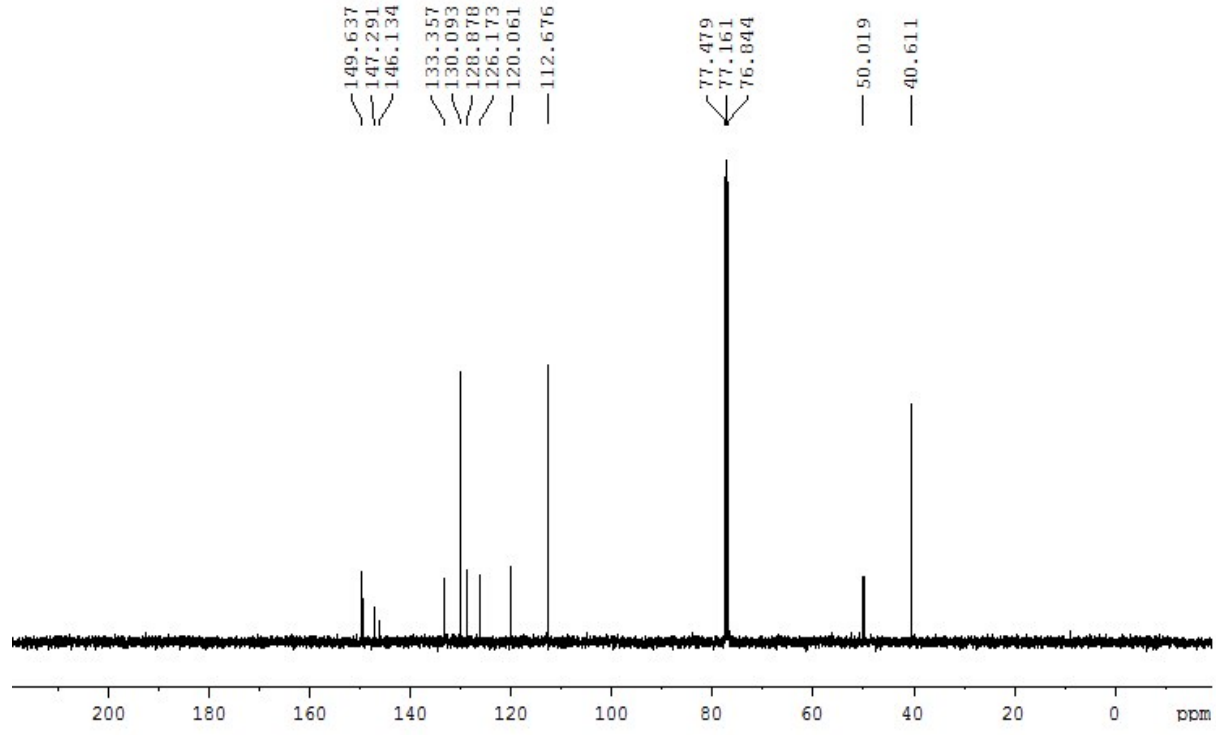

Figure S17. ^{13}C NMR spectrum (100 MHz, $CDCl_3$) of the compound **1c**

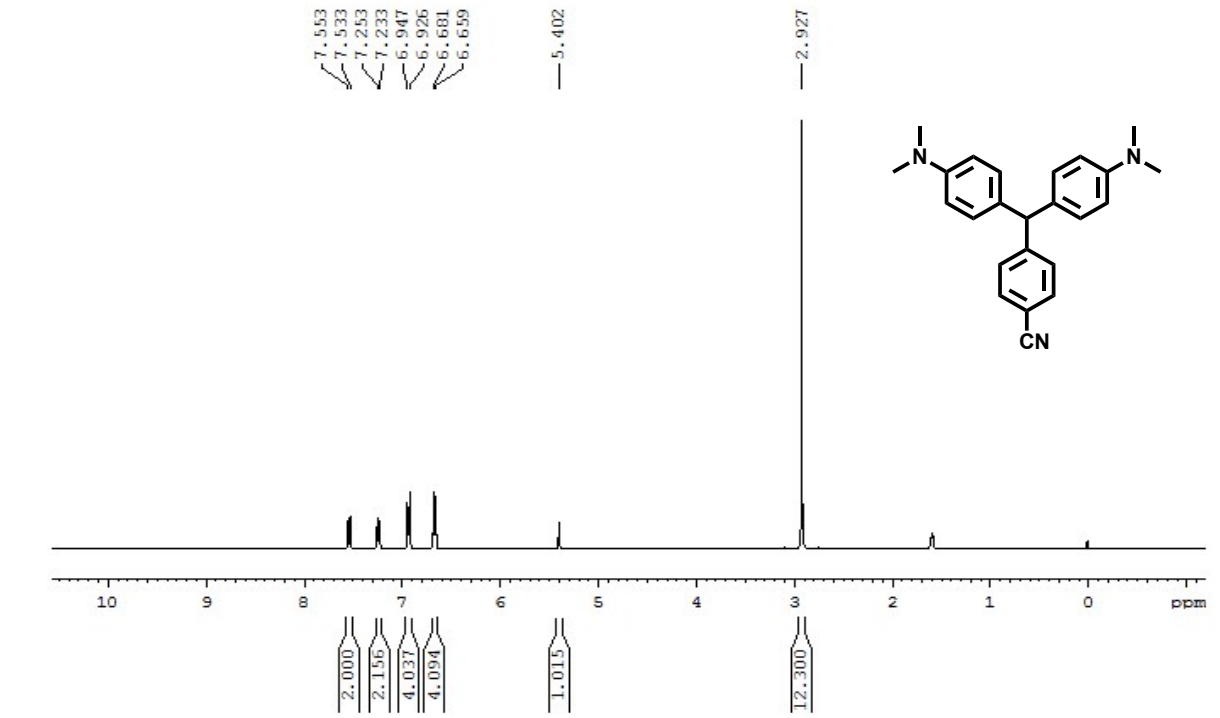

Figure S18. ^{1}H NMR spectrum (400 MHz, $CDCl_3$) of the compound **1d**

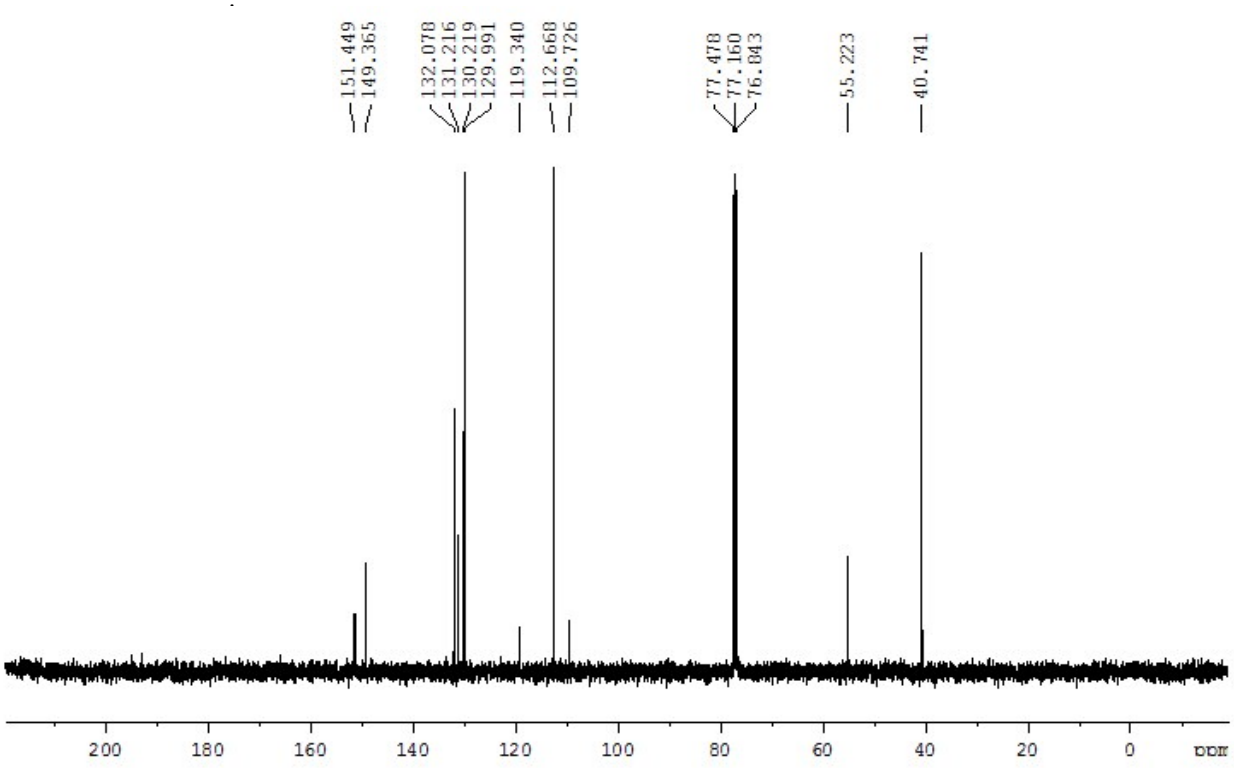

Figure S19. ^{13}C NMR spectrum (100 MHz, $CDCl_3$) of the compound **1d**

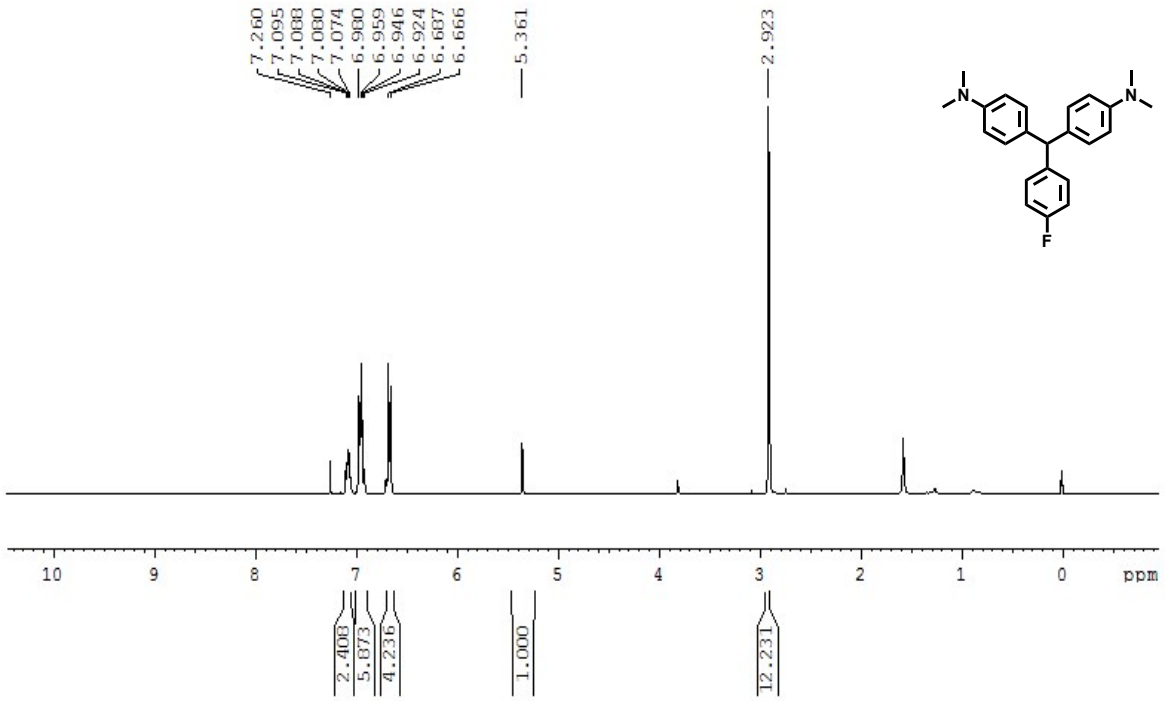

Figure S20. ^{1}H NMR spectrum (400 MHz, $CDCl_3$) of the compound **1e**

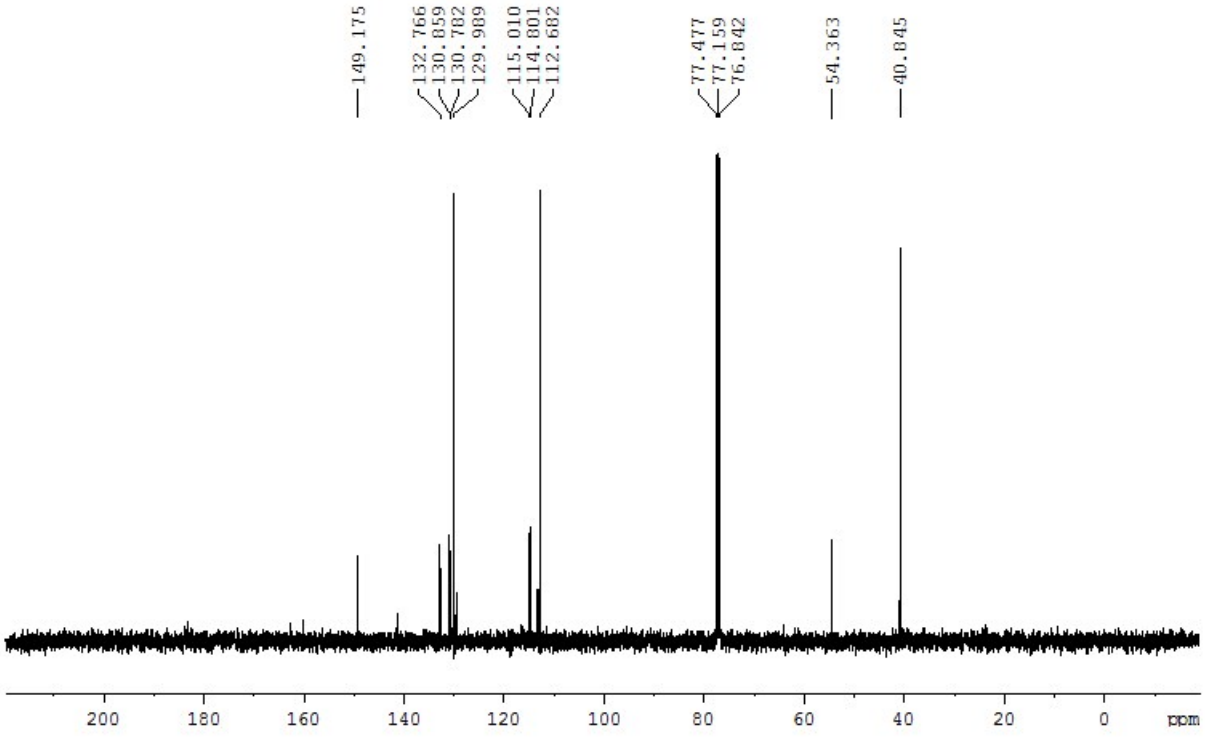

Figure S21. ^{13}C NMR spectrum (100 MHz, $CDCl_3$) of the compound **1e**

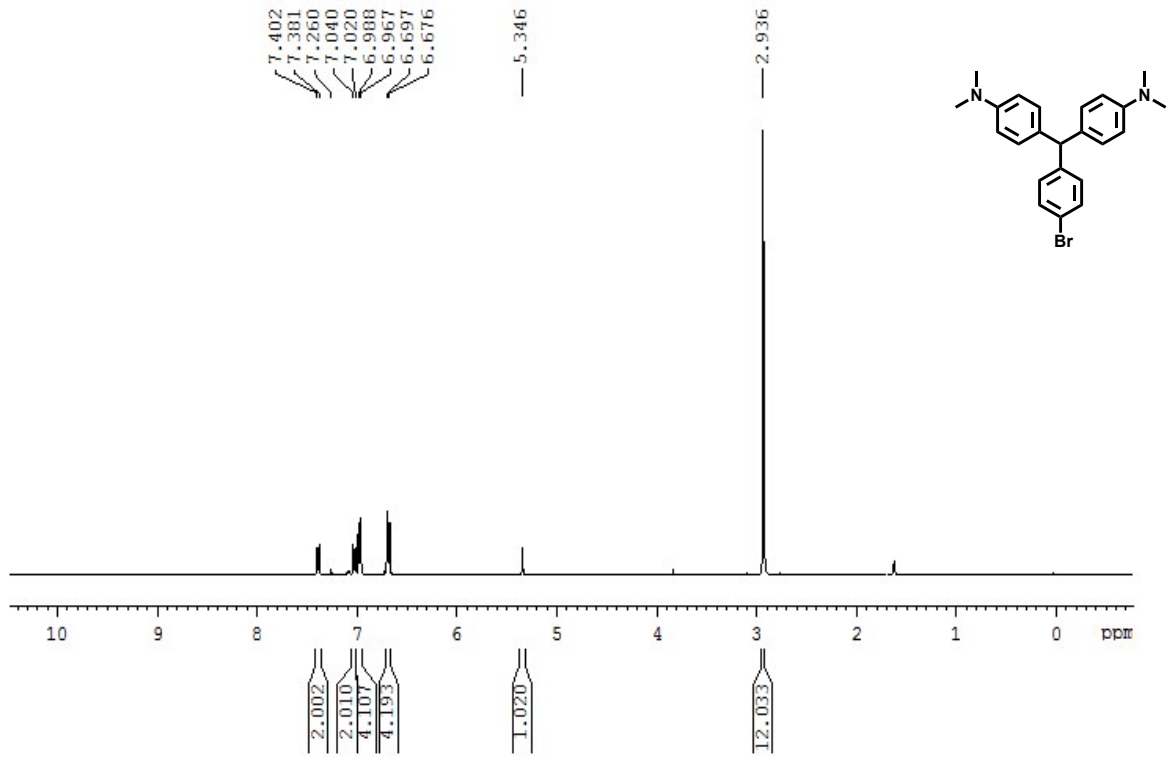

Figure S22. ^{1}H NMR spectrum (400 MHz, $CDCl_3$) of the compound **1f**

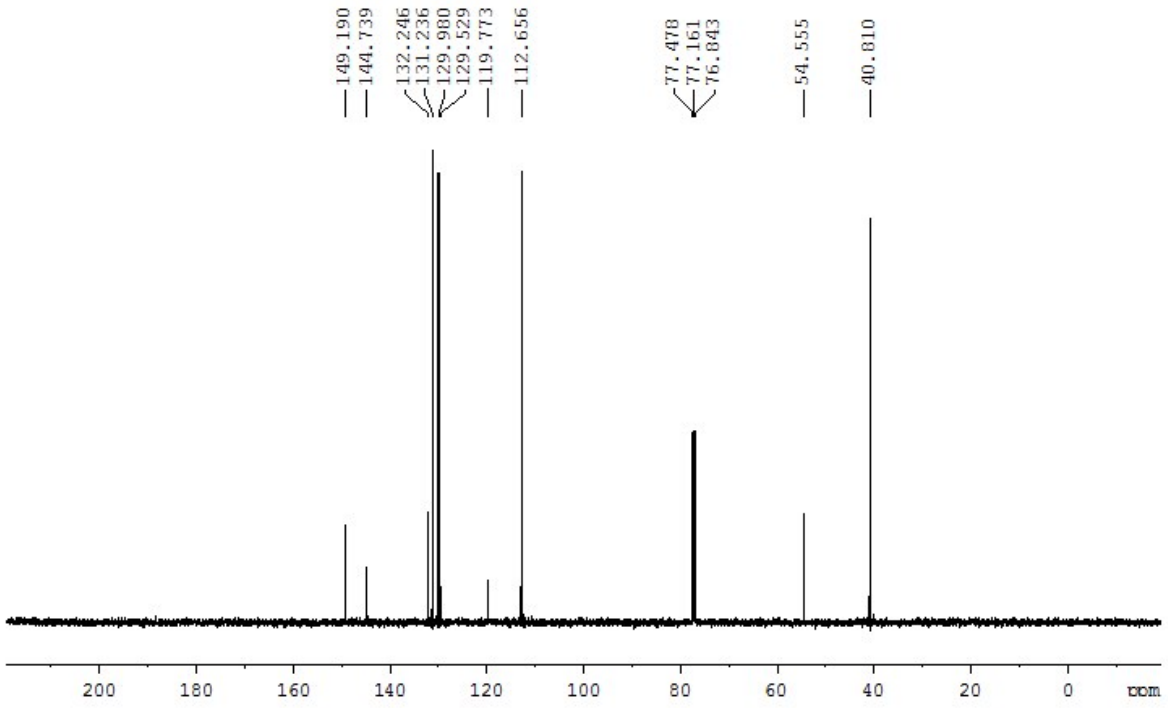

Figure S23. ^{13}C NMR spectrum (100 MHz, $CDCl_3$) of the compound **1f**

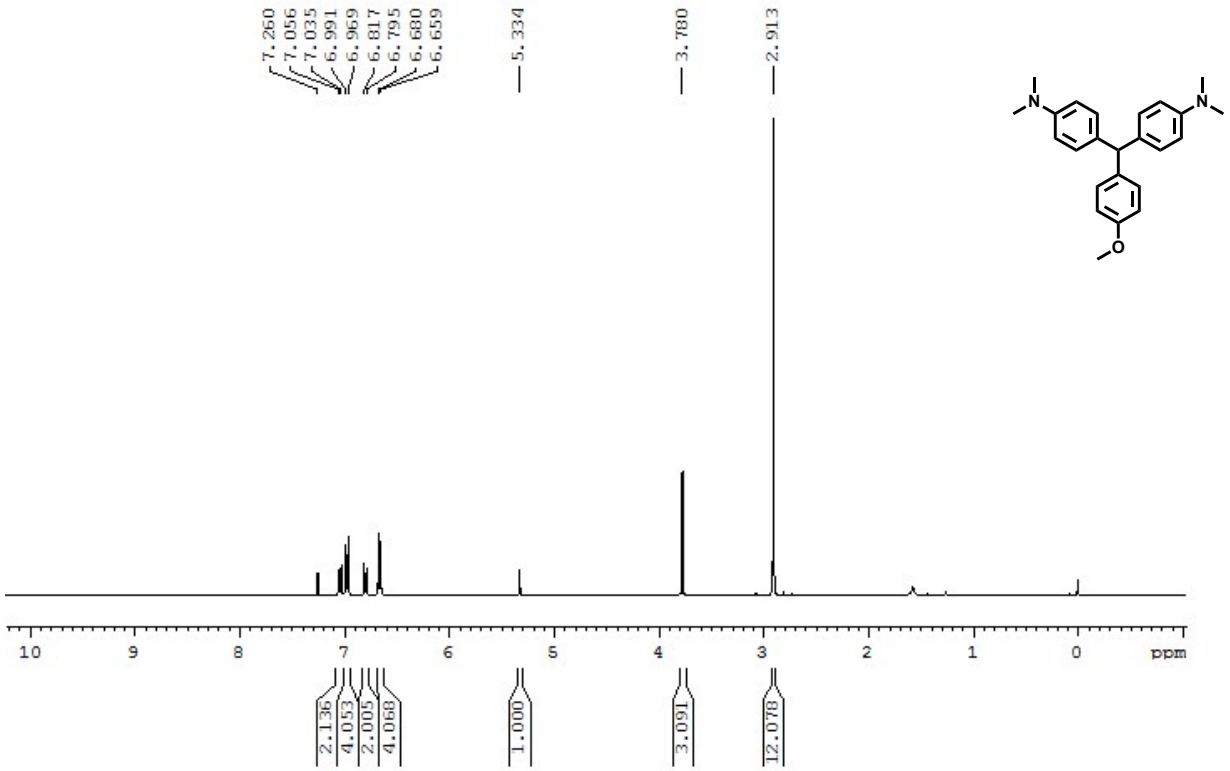

Figure S24. ^{1}H NMR spectrum (400 MHz, $CDCl_3$) of the compound **1g**

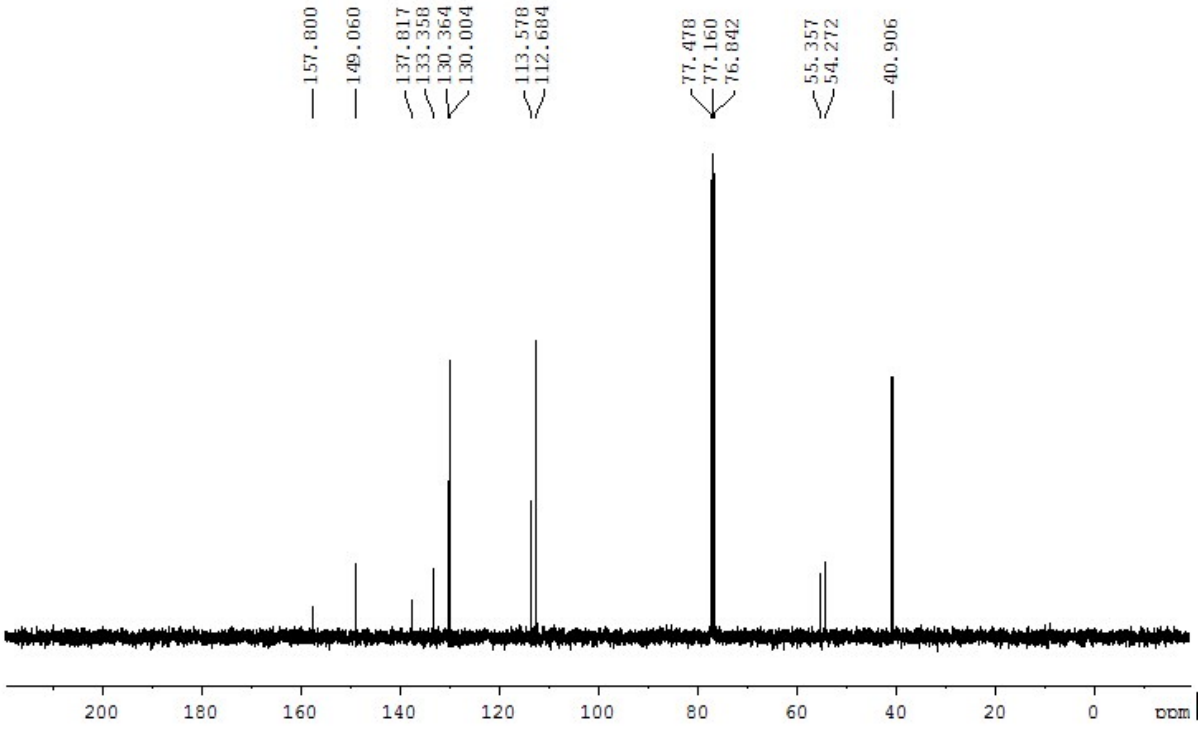

Figure S25. ^{13}C NMR spectrum (400 MHz, $CDCl_3$) of the compound **1g**

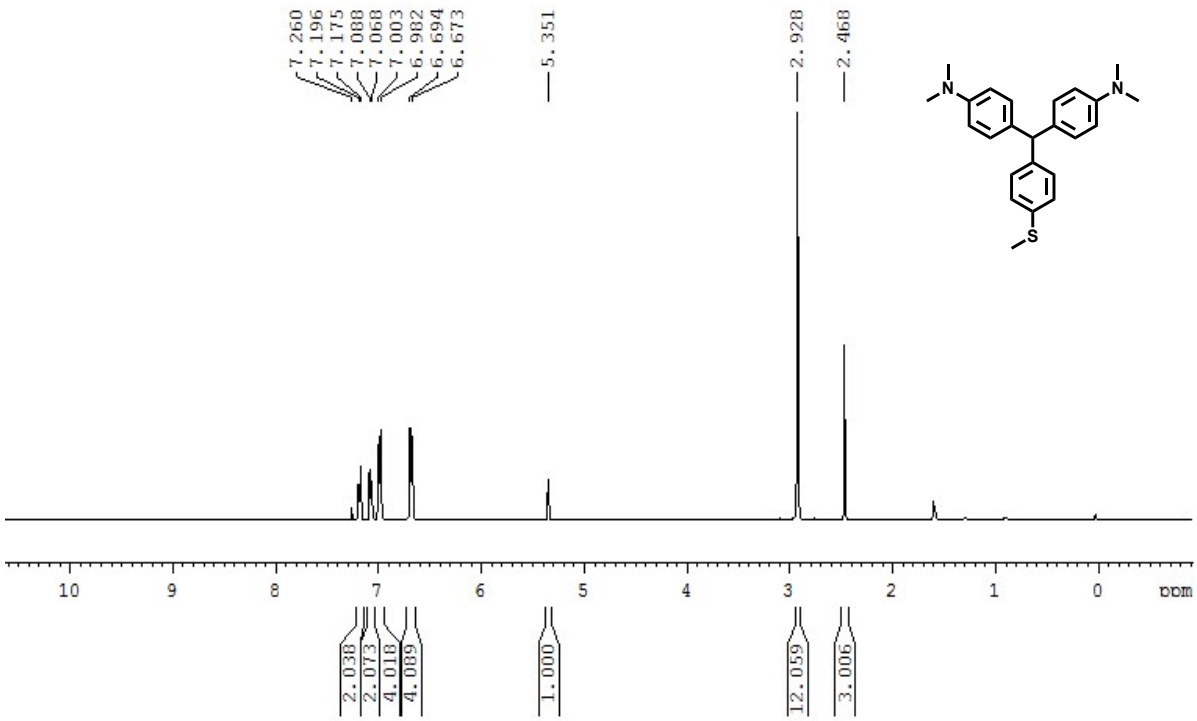

Figure S26. ^{1}H NMR spectrum (400 MHz, $CDCl_3$) of the compound **1h**

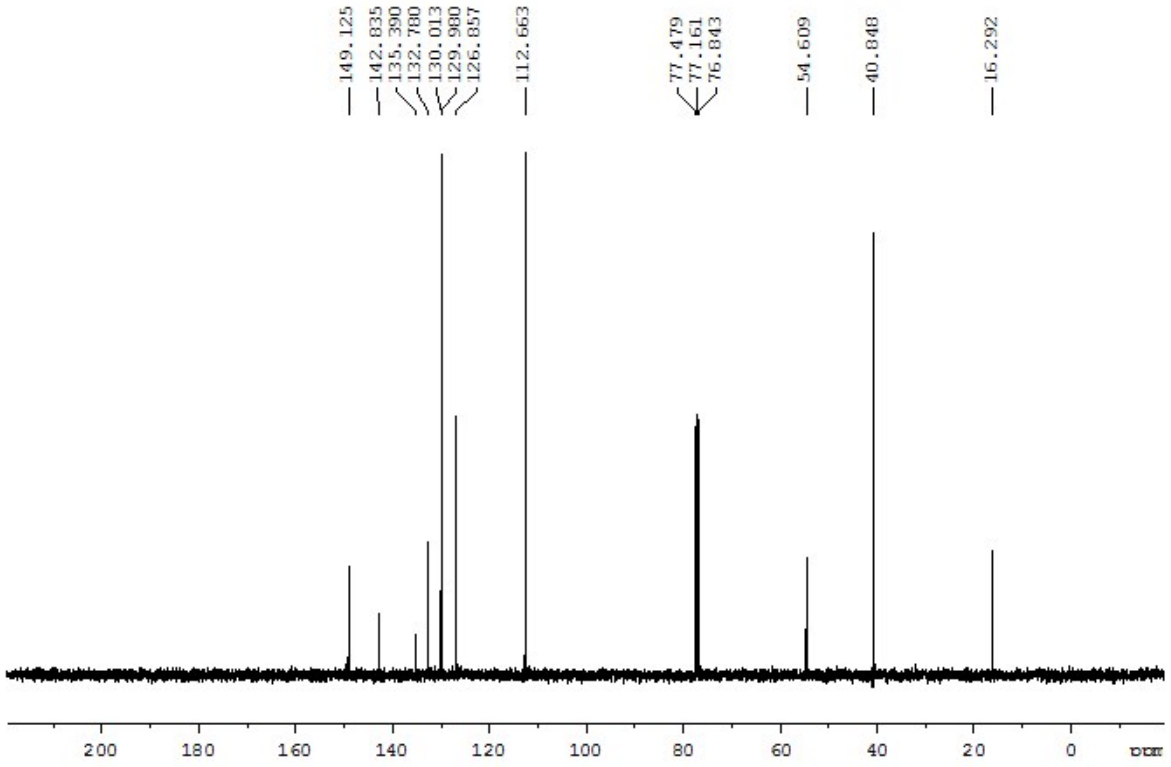

Figure S27. ^{13}C NMR spectrum (400 MHz, $CDCl_3$) of the compound **1h**

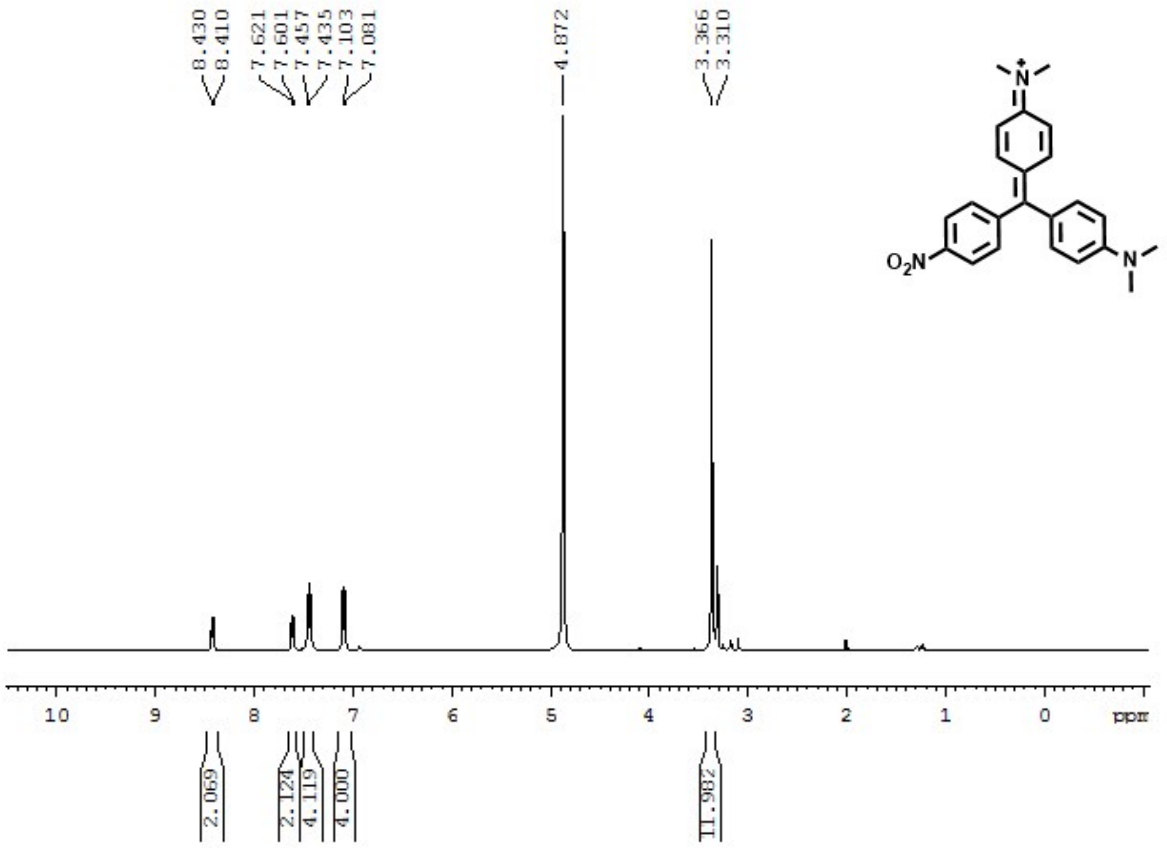

Figure S28. ^{1}H NMR spectrum (400 MHz, CD_3OD) of the compound **2b**.

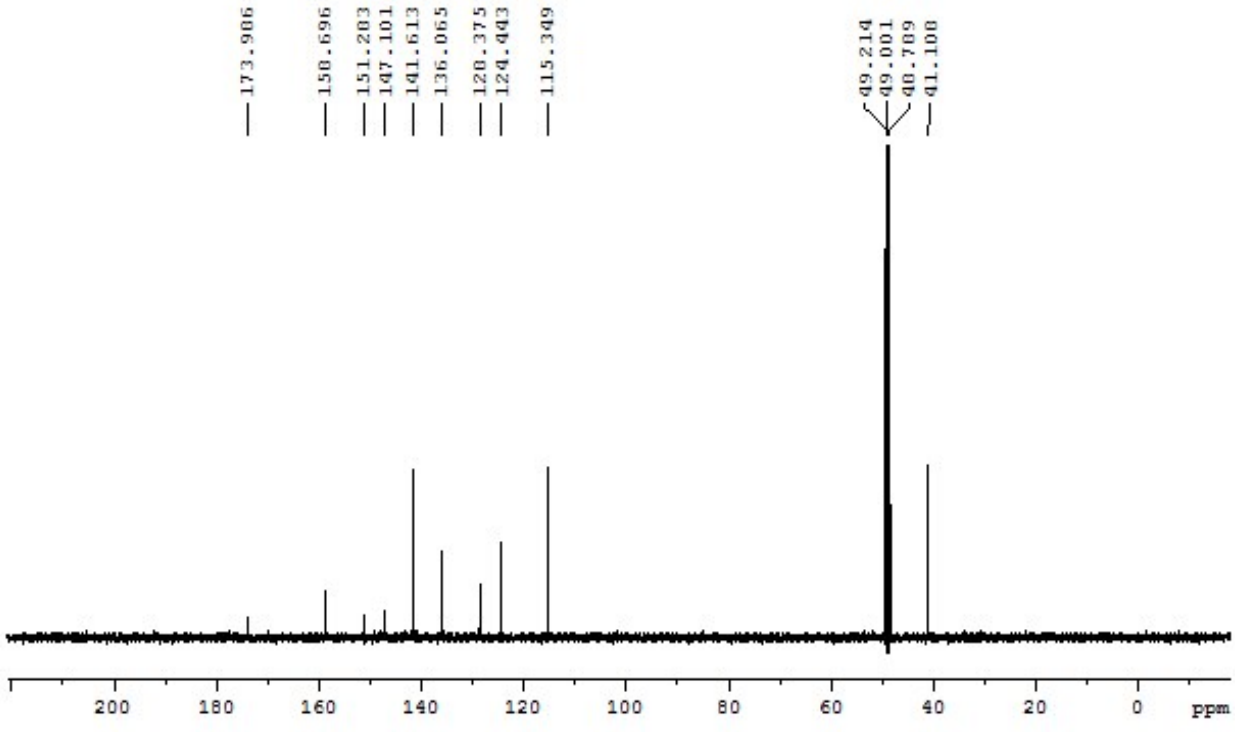

Figure S29. ^{13}C NMR spectrum (100 MHz, CD_3OD) of the compound **2b**

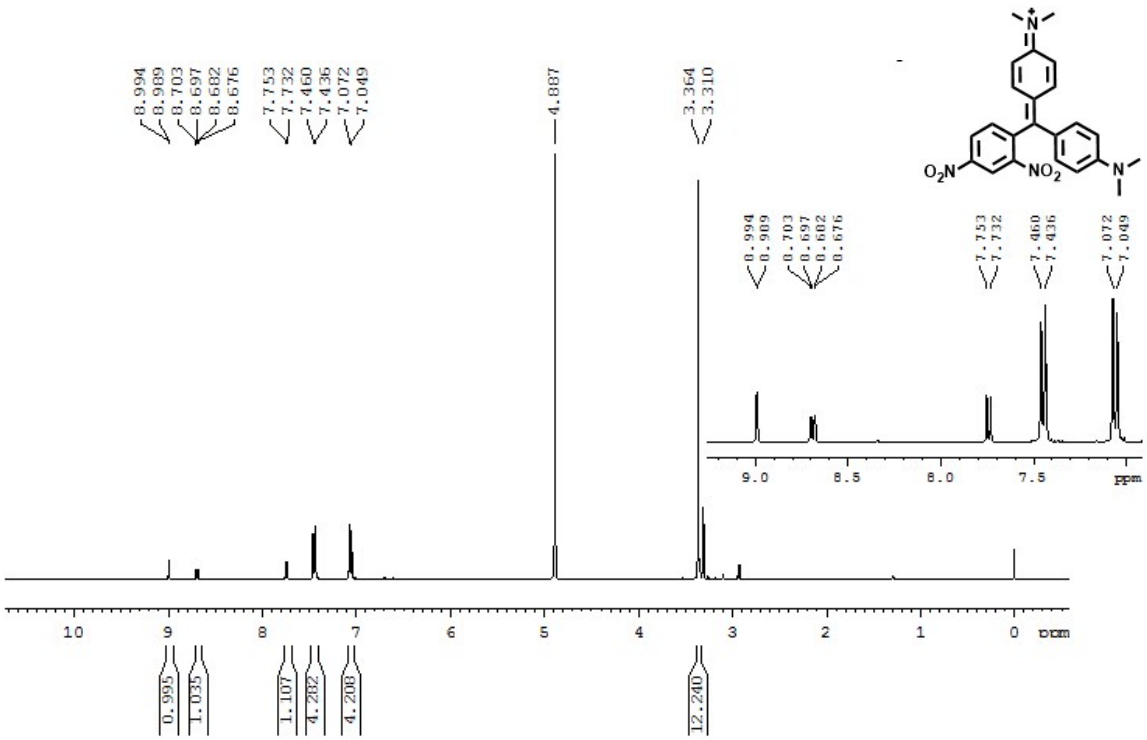

Figure S30. [1]H NMR spectrum (400 MHz, CD_3OD) of the compound **2c**.

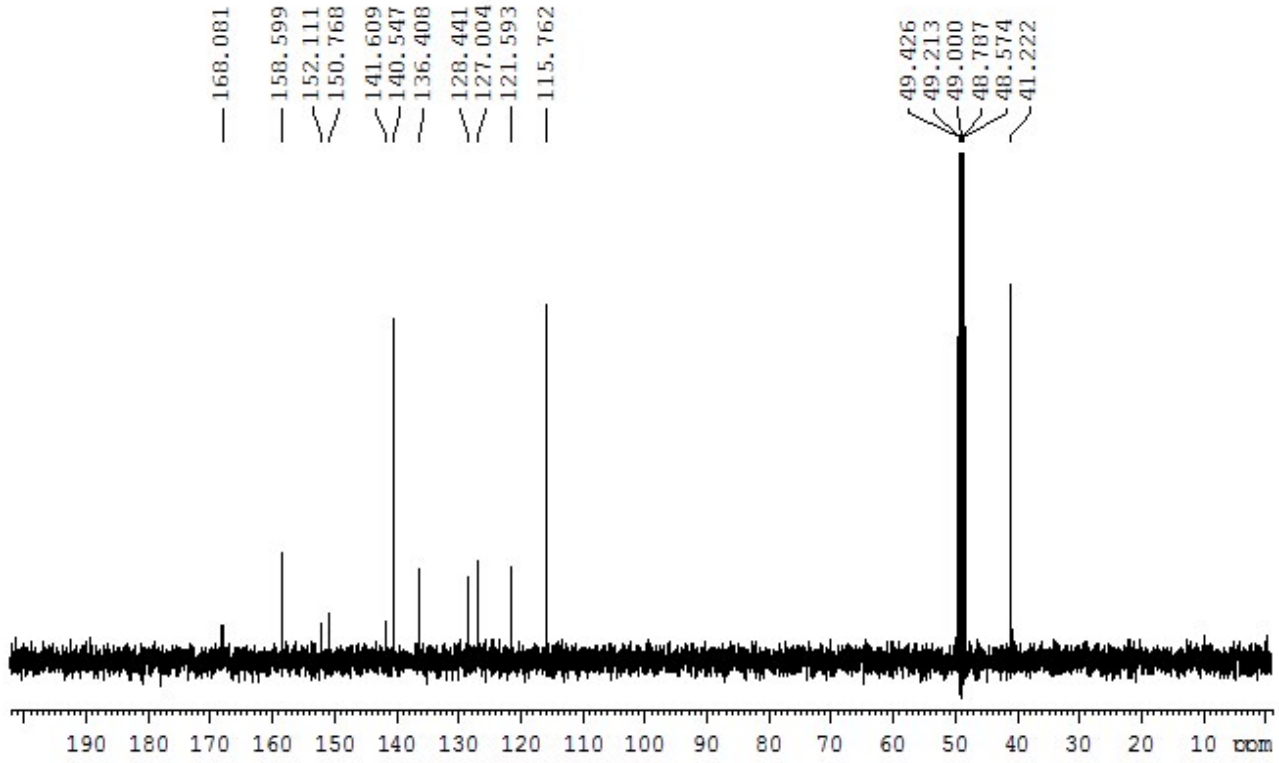

Figure S31. [13]C NMR spectrum (100 MHz, CD_3OD) of the compound **2c**

Figure S32. ^{1}H NMR spectrum (500 MHz, CD_3OD) of the compound **2d**

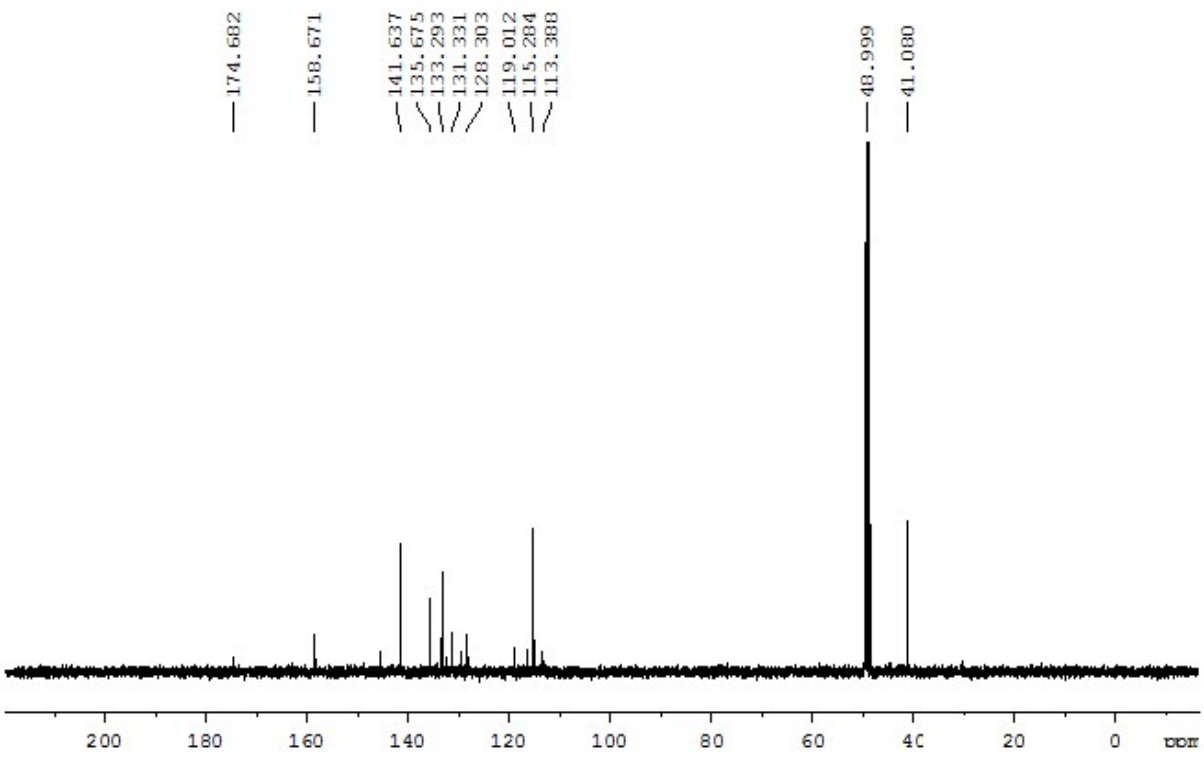

Figure S33. ^{13}C NMR spectrum (125 MHz, CD_3OD) of the compound **2d**

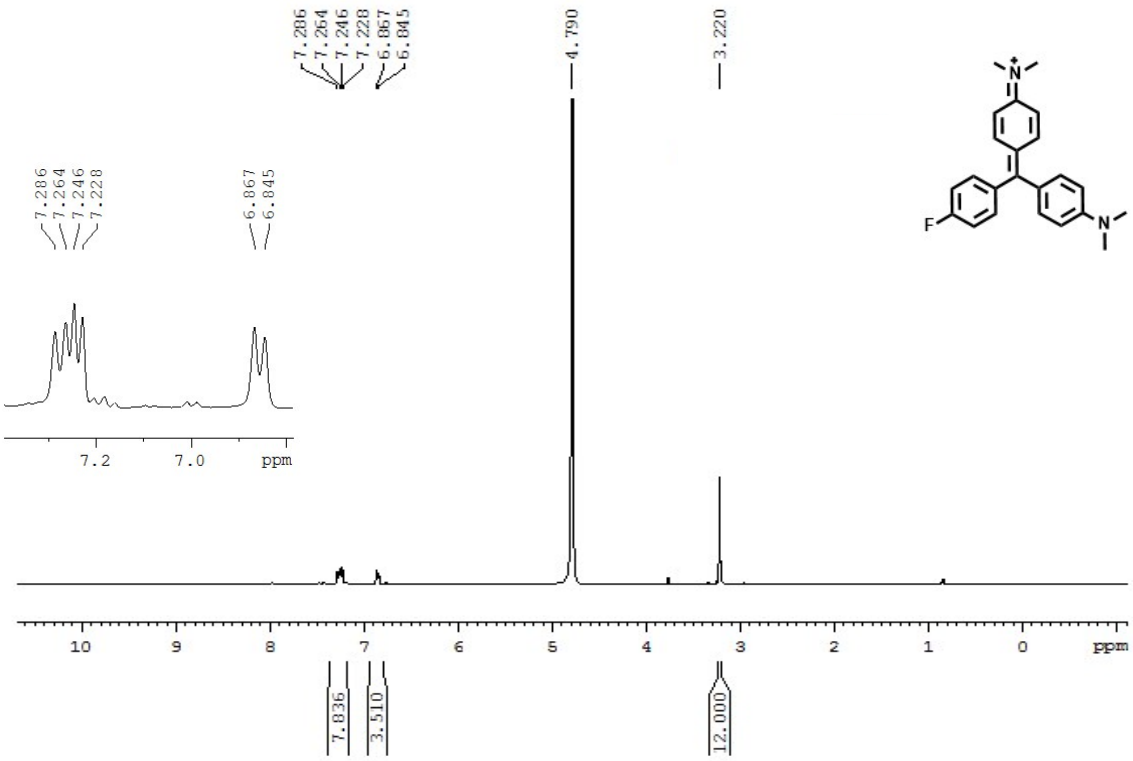

Figure S34. ^{1}H NMR spectrum (400 MHz, D_2O) of the compound **2e**.

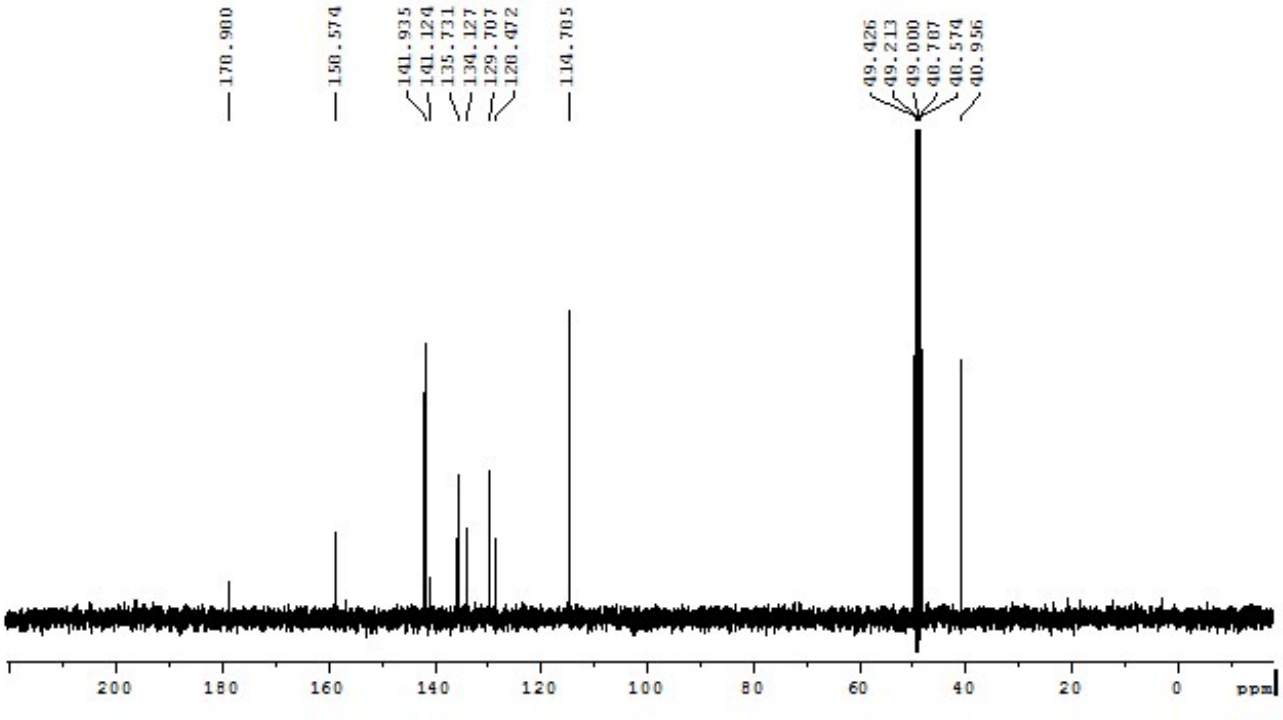

Figure S35. ^{13}C NMR spectrum (100 MHz, CD_3OD) of the compound **2e**

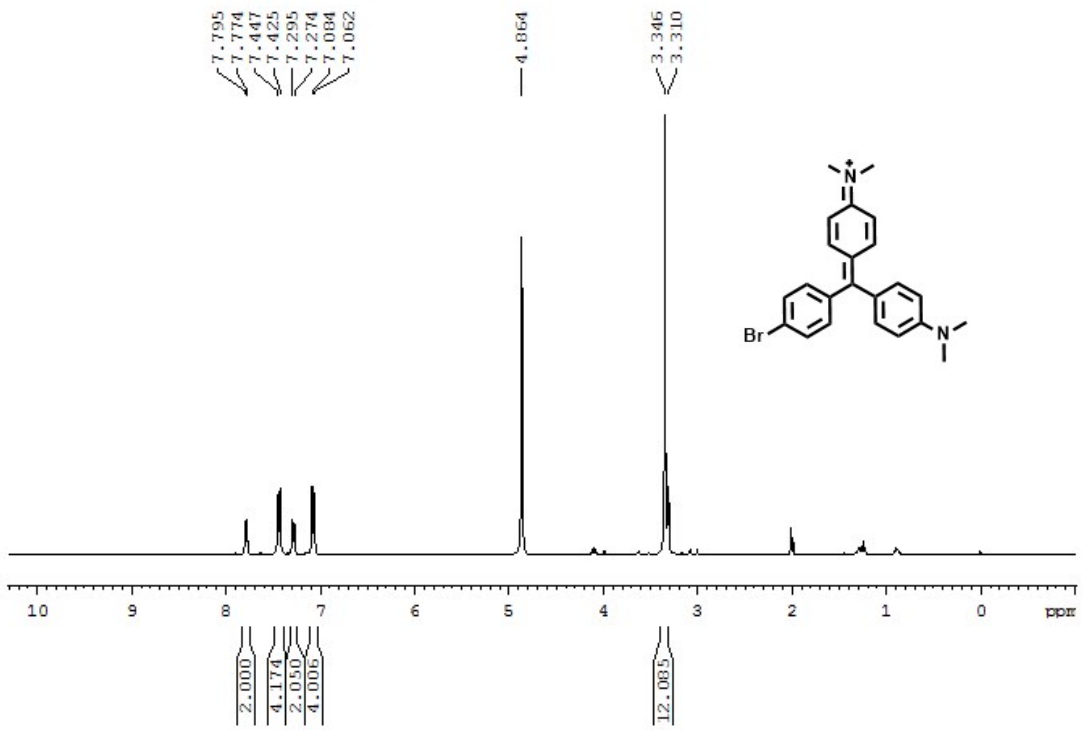

Figure S36. [1]H NMR spectrum (400 MHz, CD_3OD) of the compound **2f**

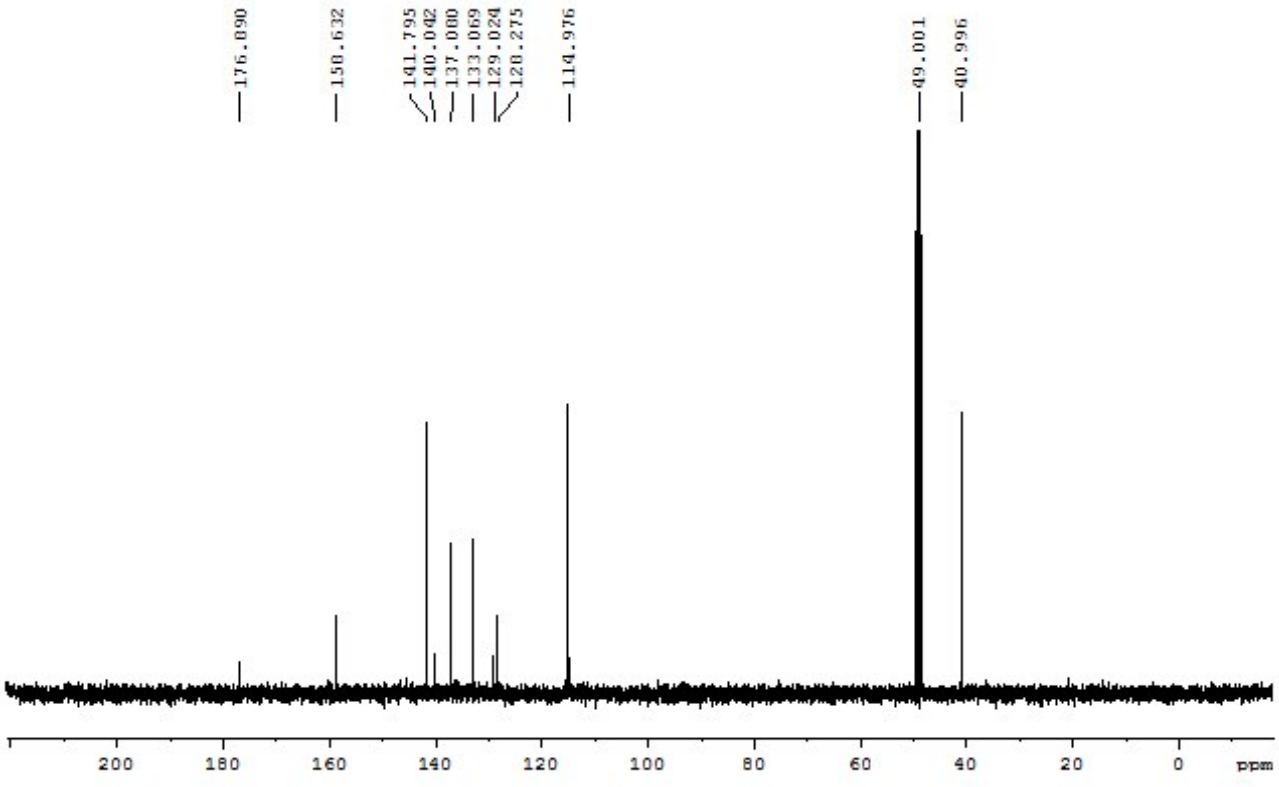

Figure S37. [13]C NMR spectrum (100 MHz, CD_3OD) of the compound **2f**

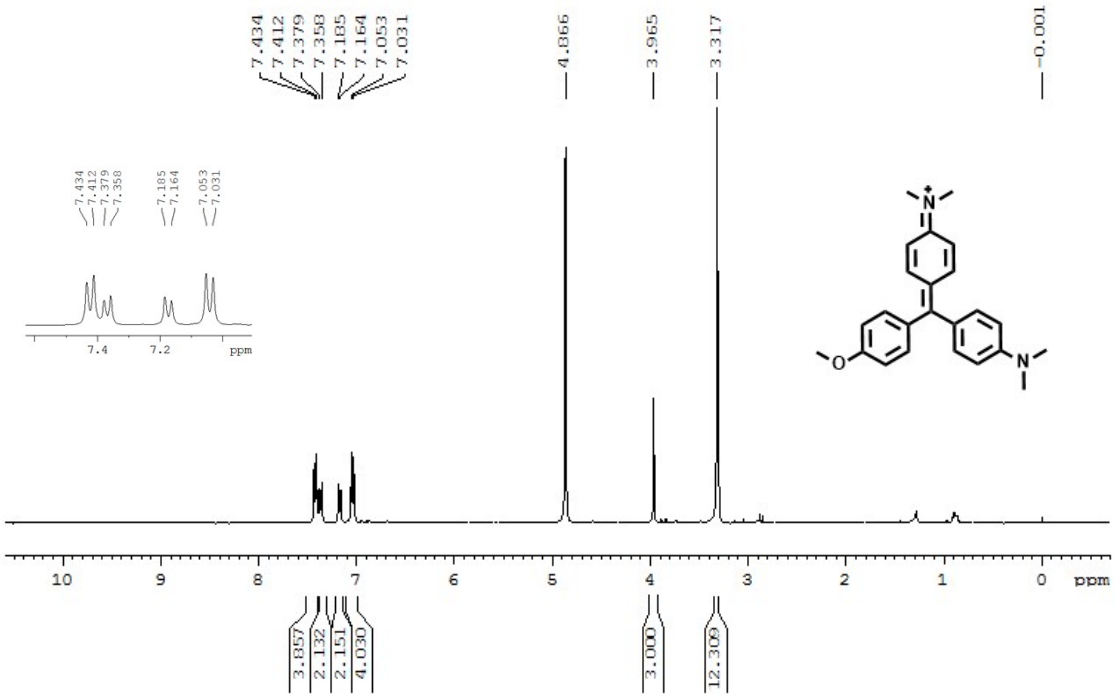

Figure S38. ^{1}H NMR spectrum (400 MHz, CD_3OD) of the compound **2g**

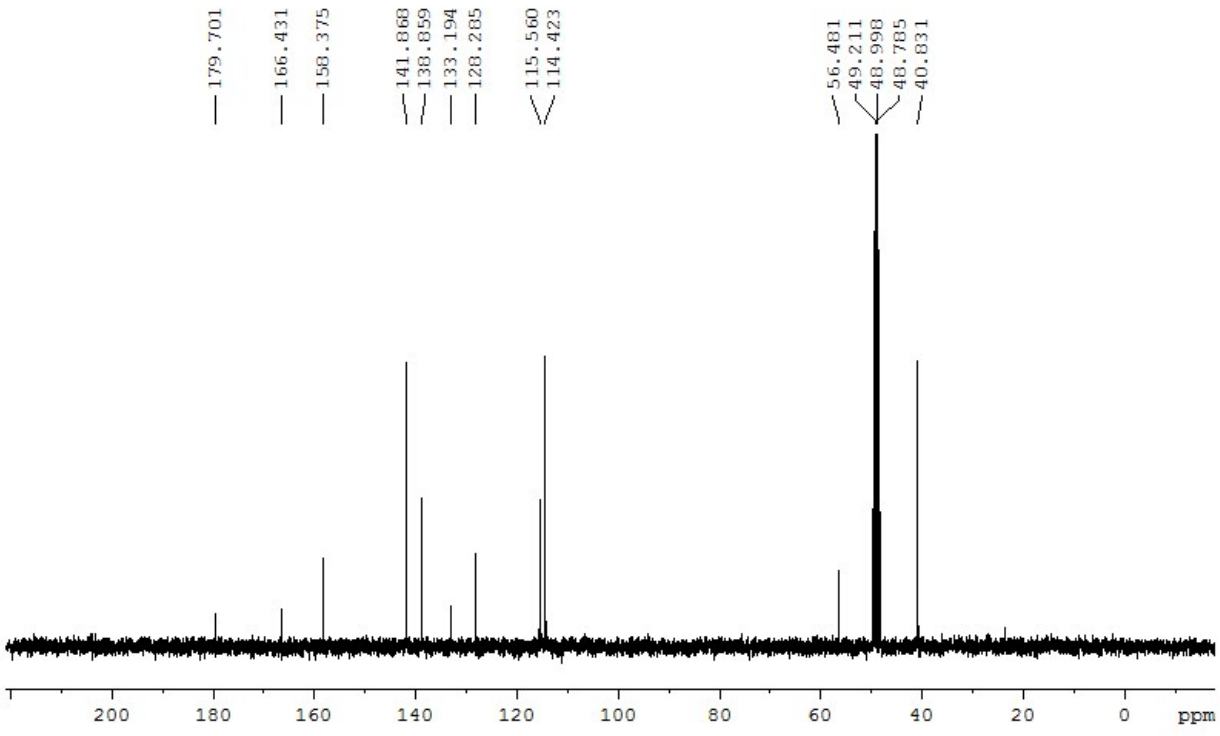

Figure S39. ^{13}C NMR spectrum (100 MHz, CD_3OD) of the compound **2g**

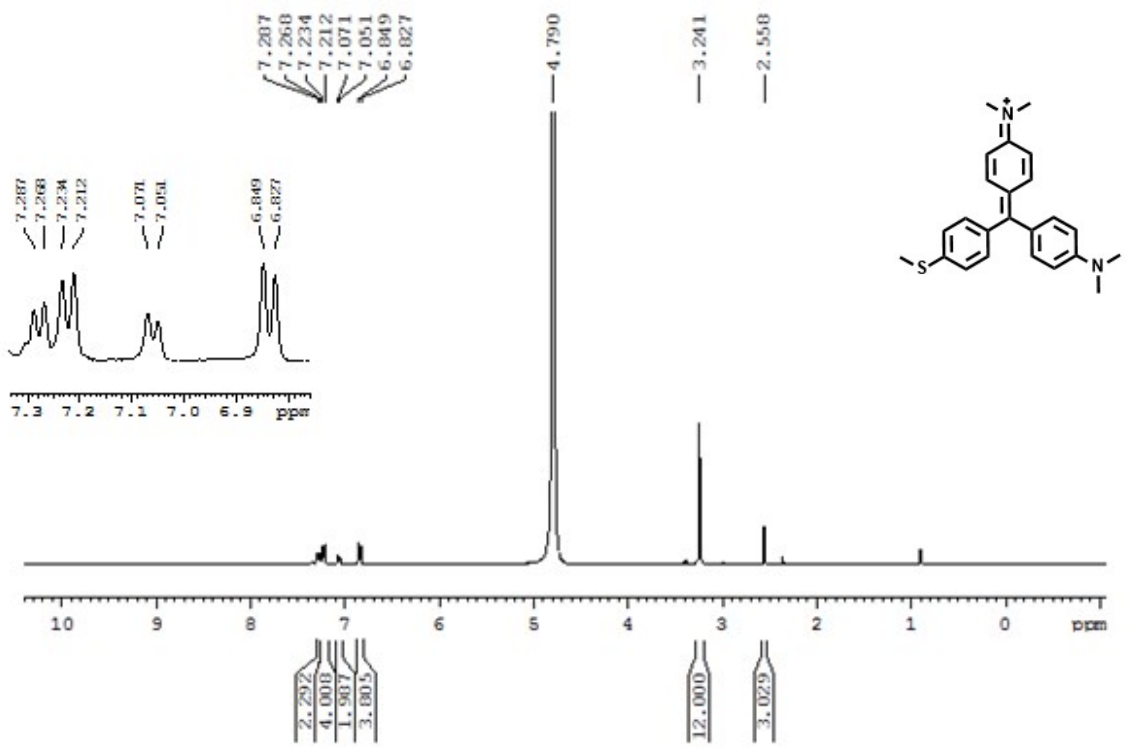

Figure S40. ^{1}H NMR spectrum (400 MHz, D_2O) of the compound **2h**

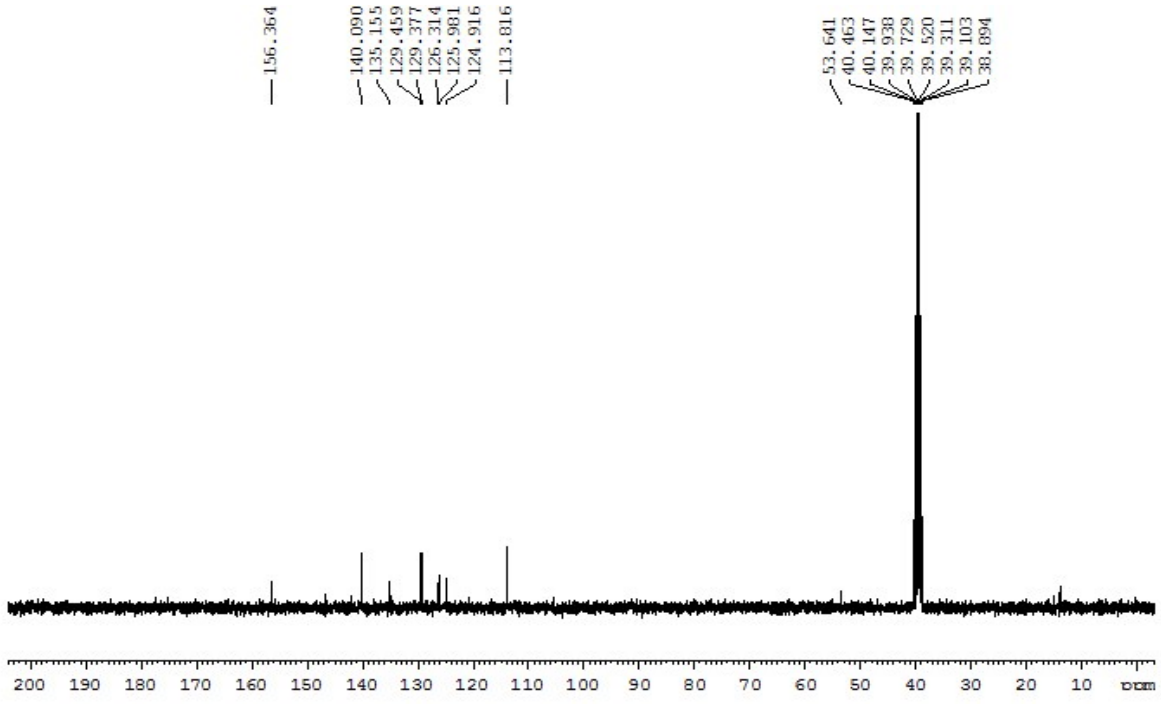

Figure S41. ^{13}C NMR spectrum (100 MHz, DMSO-d_6) of the compound **2h**

Mass spectra of compounds **2b-2h**

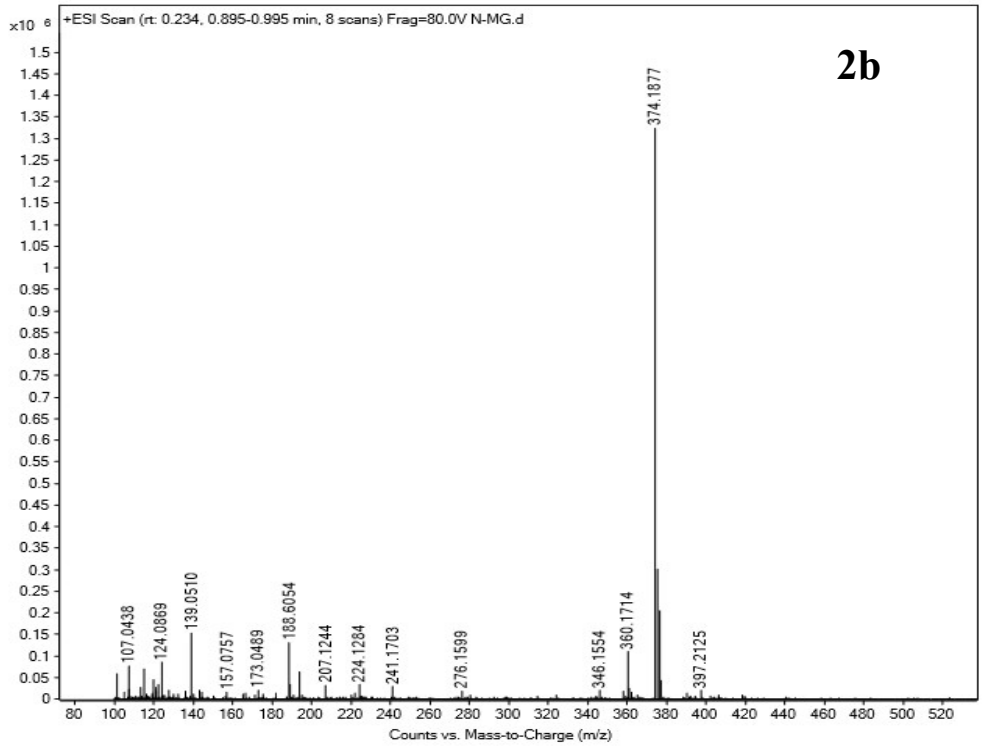

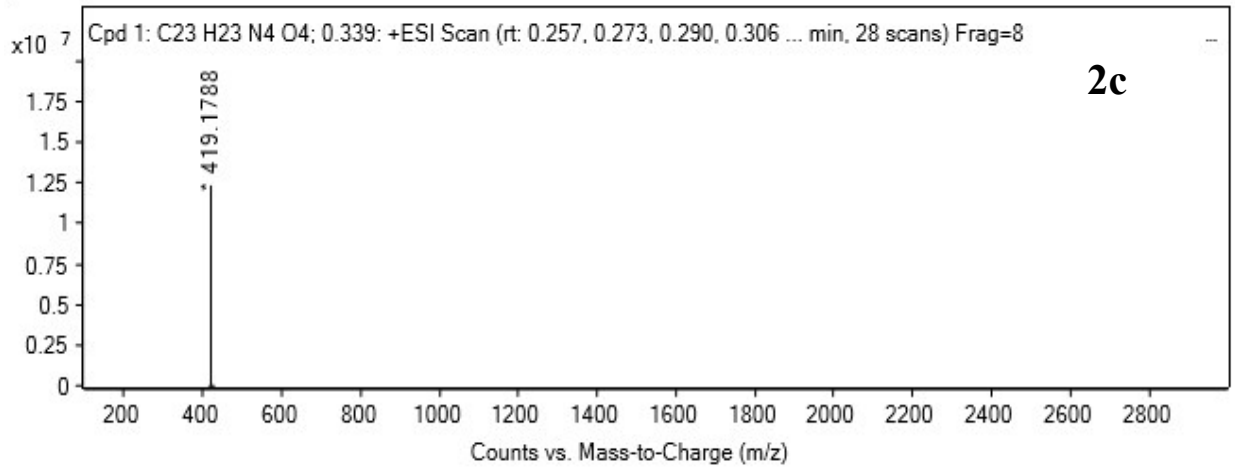

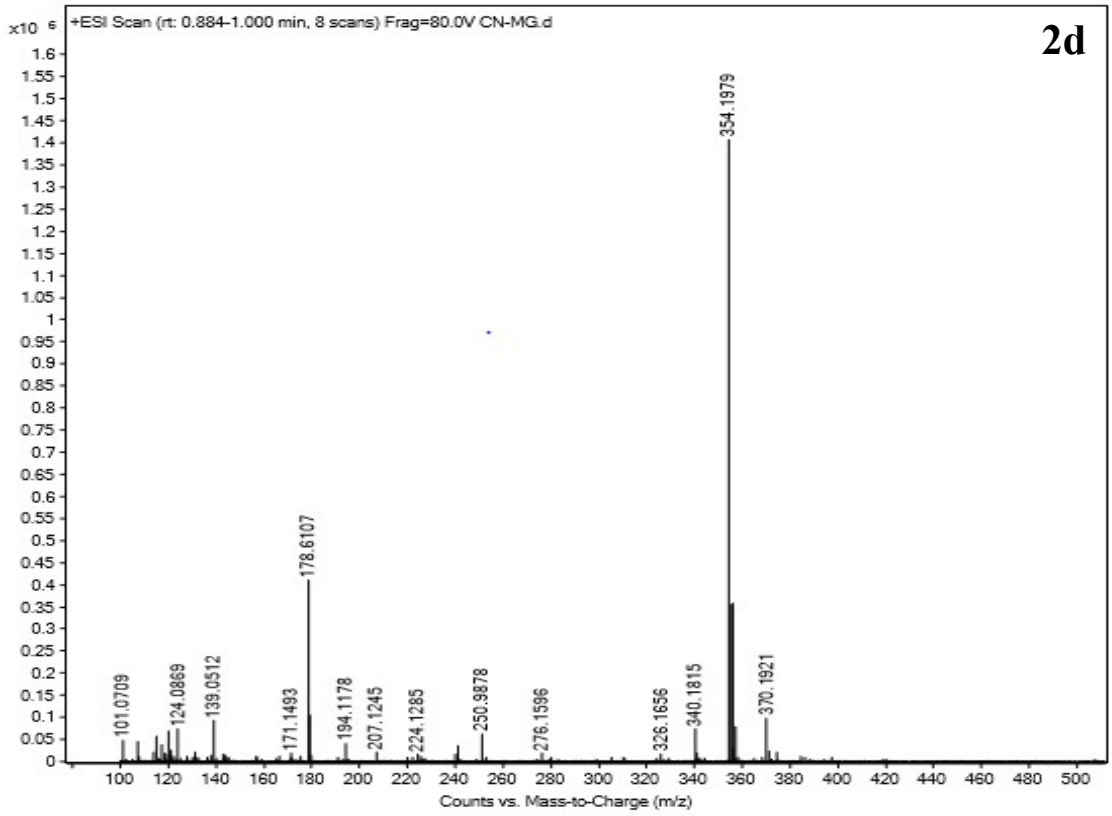
+ESI Scan (rt: 0.884-1.000 min, 8 scans) Frag=80.0V CN-MG.d
x10 6
2d
354.1979
178.6107
101.0709
124.0869
139.0512
171.1493
194.1178
207.1245
224.1285
250.9878
276.1596
326.1656
340.1815
370.1921
Counts vs. Mass-to-Charge (m/z)

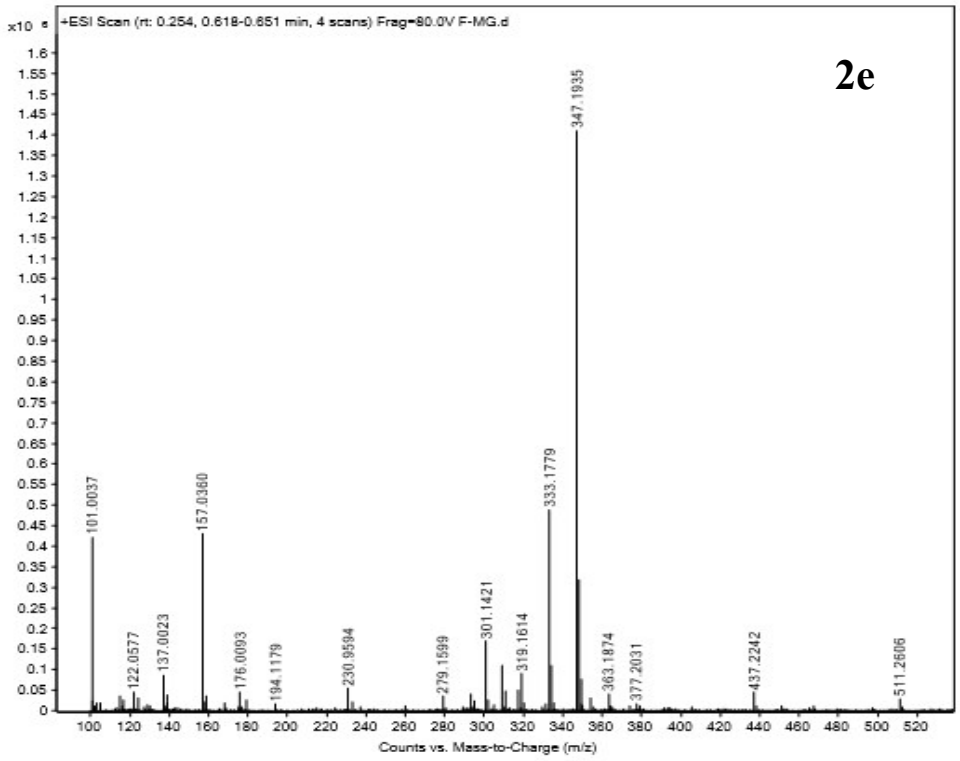
+ESI Scan (rt: 0.254, 0.618-0.651 min, 4 scans) Frag=80.0V F-MG.d
x10 6
2e
347.1935
333.1779
157.0360
101.0037
301.1421
319.1614
137.0023
122.0577
176.0093
194.1179
230.9594
279.1599
363.1874
377.2031
437.2242
511.2606
Counts vs. Mass-to-Charge (m/z)

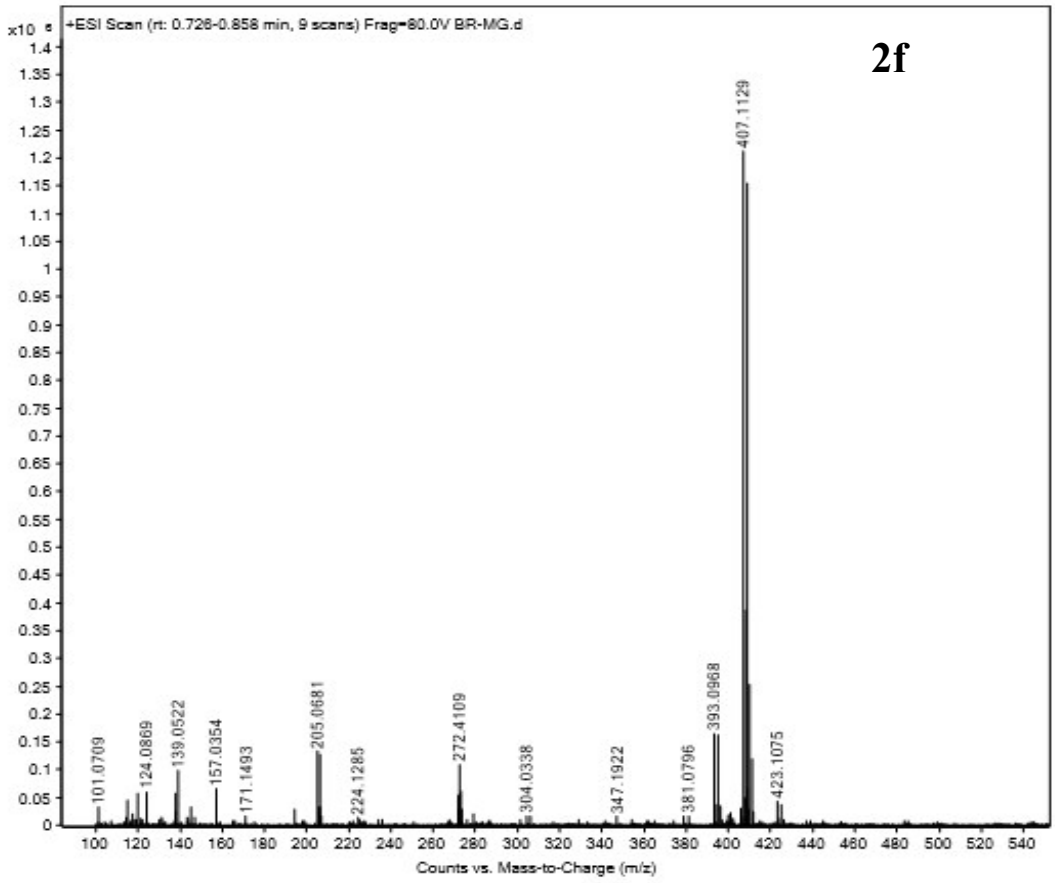
+ESI Scan (rt: 0.728-0.858 min, 9 scans) Frag=80.0V BR-MG.d
2f
x10 6
407.1129
393.0968
205.0681
272.4109
139.0522
124.0869
101.0709
157.0354
171.1493
224.1285
304.0338
347.1922
381.0796
423.1075
Counts vs. Mass-to-Charge (m/z)

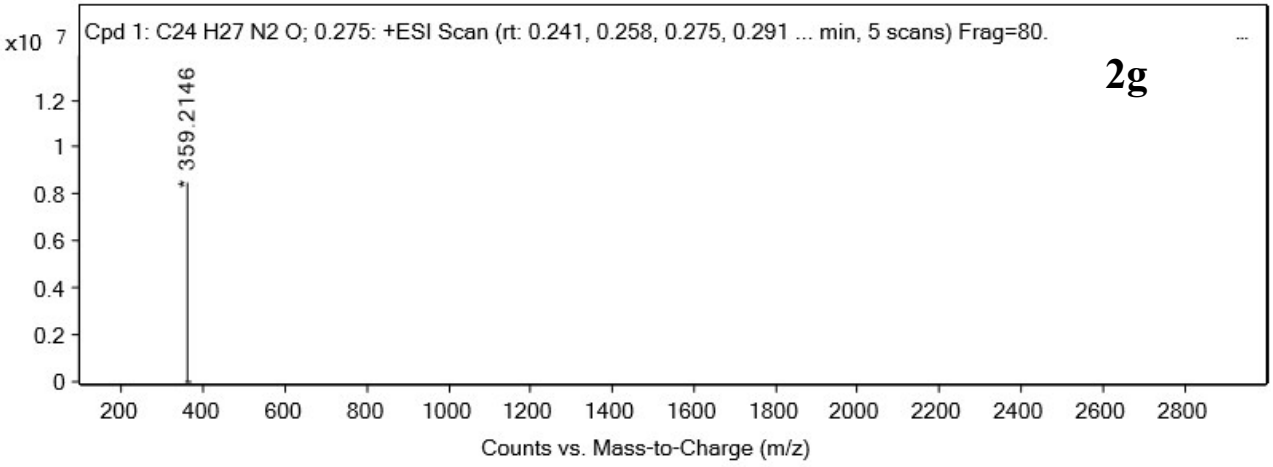
Cpd 1: C24 H27 N2 O; 0.275: +ESI Scan (rt: 0.241, 0.258, 0.275, 0.291 ... min, 5 scans) Frag=80.
2g
x10 7
359.2146
Counts vs. Mass-to-Charge (m/z)

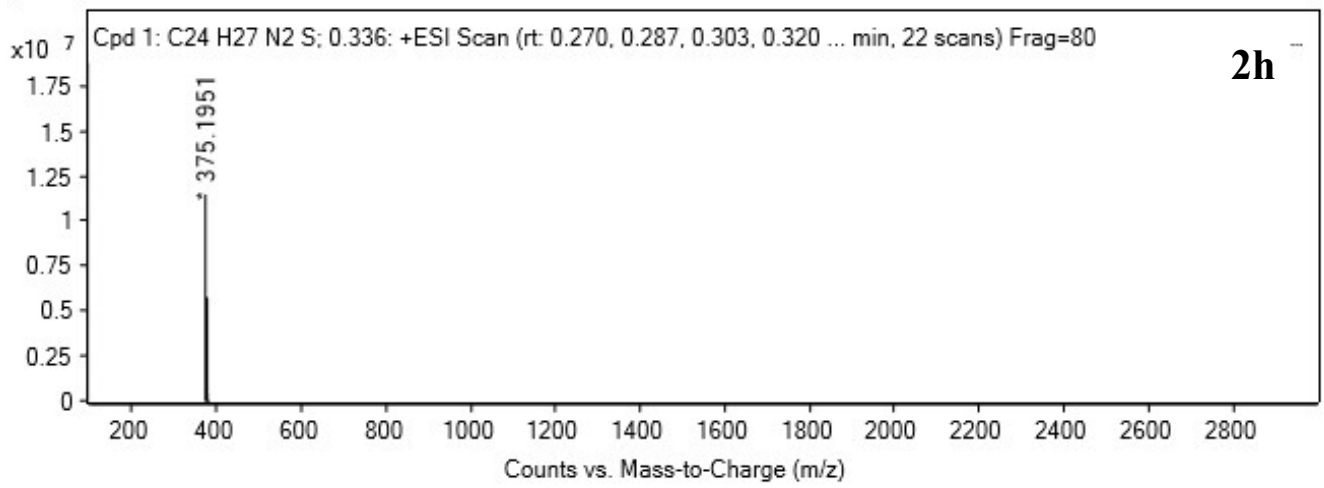
Cpd 1: C24 H27 N2 S; 0.336: +ESI Scan (rt: 0.270, 0.287, 0.303, 0.320 ... min, 22 scans) Frag=80
2h
x10 7
1.75
1.5
1.25
1
0.75
0.5
0.25
0
375.1951
200
400
600
800
1000
1200
1400
1600
1800
2000
2200
2400
2600
2800
Counts vs. Mass-to-Charge (m/z)